

DG method II: PDEs with higher order derivatives

Chi-Wang Shu

Division of Applied Mathematics
Brown University

FlowModellium Lab, MIPT, September 2013

Outline

- Introduction
- LDG method for convection diffusion equations
- Other DG methods for diffusion equations
- LDG method for KdV equations
- LDG methods for other higher order diffusion and dispersive wave equations

- Recent development and applications:
 1. Positivity-preserving finite volume and DG method
 2. Multiscale DG method for solving elliptic problems with curvilinear unidirectional rough coefficients
 3. Energy conserving LDG methods for second order wave equations

Introduction

A naive generalization of the DG method to a PDE containing higher order spatial derivatives could have disastrous results.

Consider, as a simple example, the heat equation

$$u_t - u_{xx} = 0 \tag{1}$$

for $x \in [0, 2\pi]$ with periodic boundary conditions and with an initial condition $u(x, 0) = \sin(x)$.

A straightforward generalization of the DG method from the hyperbolic equation $u_t + f(u)_x = 0$ is to write down the same scheme and replace $f(u)$ by $-u_x$ everywhere: find $u \in V_h$ such that, for all test functions $v \in V_h$,

$$\int_{I_j} u_t v dx + \int_{I_j} u_x v_x dx - \hat{u}_{xj+\frac{1}{2}}^- v_{j+\frac{1}{2}}^- + \hat{u}_{xj-\frac{1}{2}}^+ v_{j-\frac{1}{2}}^+ = 0 \quad (2)$$

Lacking an upwinding consideration for the choice of the flux \hat{u}_x and considering that diffusion is isotropic, a natural choice for the flux could be the central flux

$$\hat{u}_{xj+\frac{1}{2}} = \frac{1}{2} \left((u_x)_{j+\frac{1}{2}}^- + (u_x)_{j+\frac{1}{2}}^+ \right)$$

However the result is horrible!

Table 1: L^2 and L^∞ errors and orders of accuracy for the “inconsistent” discontinuous Galerkin method (2) applied to the heat equation (1) with an initial condition $u(x, 0) = \sin(x)$, $t = 0.8$. Third order Runge-Kutta in time.

| Δx | $k = 1$ | | | | | $k = 2$ | | | | |
|------------|-------------|-------|------------------|-------|--|-------------|-------|------------------|-------|--|
| | L^2 error | order | L^∞ error | order | | L^2 error | order | L^∞ error | order | |
| $2\pi/20$ | 1.78E-01 | — | 2.58E-01 | — | | 1.85E-01 | — | 2.72E-01 | — | |
| $2\pi/40$ | 1.76E-01 | 0.016 | 2.50E-01 | 0.025 | | 1.78E-01 | 0.049 | 2.55E-01 | 0.089 | |
| $2\pi/80$ | 1.75E-01 | 0.004 | 2.48E-01 | 0.012 | | 1.77E-01 | 0.013 | 2.51E-01 | 0.025 | |
| $2\pi/160$ | 1.75E-01 | 0.001 | 2.48E-01 | 0.003 | | 1.76E-01 | 0.003 | 2.50E-01 | 0.007 | |

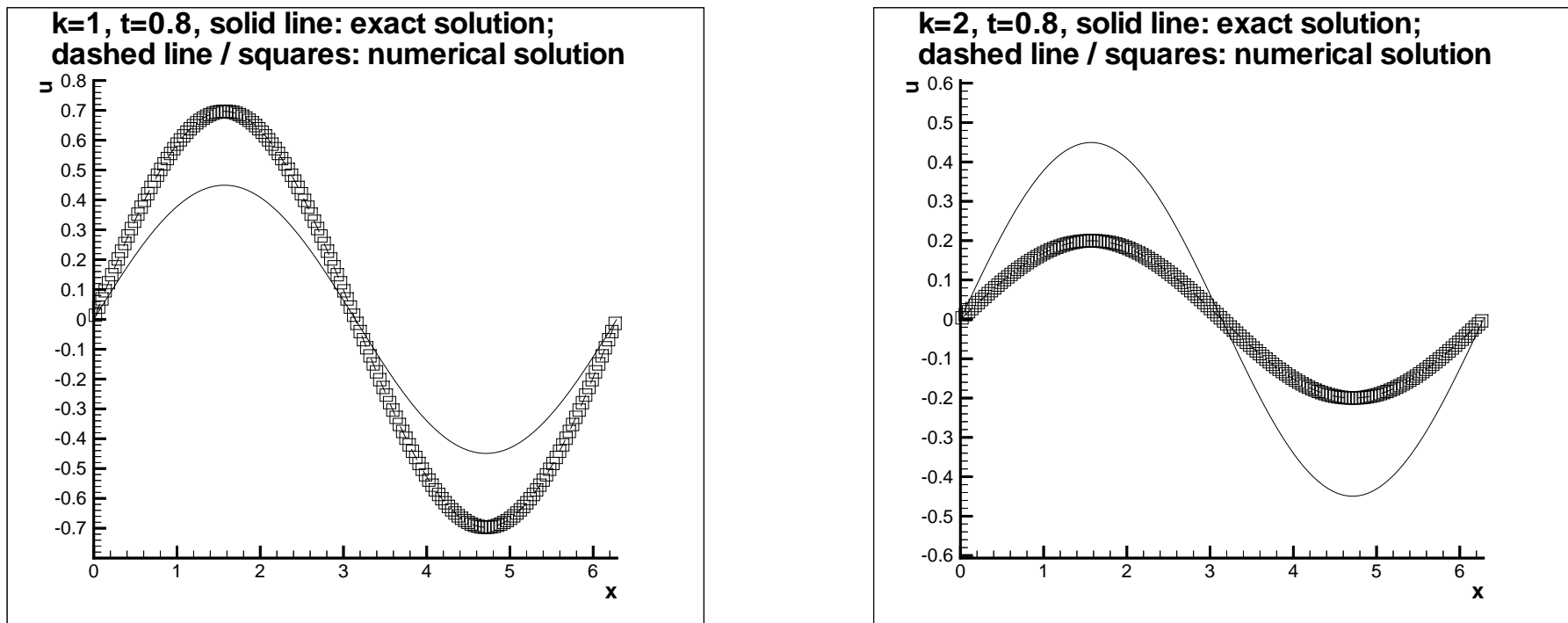


Figure 1: The “inconsistent” discontinuous Galerkin method (2) applied to the heat equation (1) with an initial condition $u(x, 0) = \sin(x)$. $t = 0.8$. 160 cells. Third order Runge-Kutta in time. Solid line: the exact solution; Dashed line and squares symbols: the computed solution at the cell centers. Left: $k = 1$; Right: $k = 2$.

It is proven in [Zhang and Shu, *M³AS* 03](#), that this "inconsistent" DG method for the heat equation is actually

- consistent with the heat equation,
- but (very weakly) unstable.

LDG method for convection diffusion equations

A good DG method for the heat equation: the local DG (LDG) method
(Bassi and Rebay, JCP 97; Cockburn and Shu, SINUM 98): rewrite the
heat equation as

$$u_t - q_x = 0, \quad q - u_x = 0, \quad (3)$$

and *formally* write out the DG scheme as: find $u, q \in V_h$ such that, for all test functions $v, w \in V_h$,

$$\int_{I_j} u_t v dx + \int_{I_j} q v_x dx - \hat{q}_{j+\frac{1}{2}} v_{j+\frac{1}{2}}^- + \hat{q}_{j-\frac{1}{2}} v_{j-\frac{1}{2}}^+ = 0 \quad (4)$$

$$\int_{I_j} q w dx + \int_{I_j} u w_x dx - \hat{u}_{j+\frac{1}{2}} w_{j+\frac{1}{2}}^- + \hat{u}_{j-\frac{1}{2}} w_{j-\frac{1}{2}}^+ = 0,$$

q can be **locally** (within cell I_j) solved and eliminated, hence **local** DG.

A key ingredient of the design of the LDG method is the choice of the numerical fluxes \hat{u} and \hat{q} (remember: no upwinding principle for guidance).

The best choice for the numerical fluxes is the following alternating flux

$$\hat{u}_{j+\frac{1}{2}} = u_{j+\frac{1}{2}}^-, \quad \hat{q}_{j+\frac{1}{2}} = q_{j+\frac{1}{2}}^+. \quad (5)$$

The other way around also works

$$\hat{u}_{j+\frac{1}{2}} = u_{j+\frac{1}{2}}^+, \quad \hat{q}_{j+\frac{1}{2}} = q_{j+\frac{1}{2}}^-.$$

We then have

- L^2 stability
- optimal convergence of $O(h^{k+1})$ in L^2 for P^k elements

Table 2: L^2 and L^∞ errors and orders of accuracy for the LDG applied to the heat equation.

| | $k = 1$ | | | | $k = 2$ | | | |
|---------------|-------------|-------|------------------|-------|-------------|-------|------------------|-------|
| Δx | L^2 error | order | L^∞ error | order | L^2 error | order | L^∞ error | order |
| $2\pi/20, u$ | 1.92E-03 | — | 7.34E-03 | — | 4.87E-05 | — | 2.30E-04 | — |
| $2\pi/20, q$ | 1.93E-03 | — | 7.33E-03 | — | 4.87E-05 | — | 2.30E-04 | — |
| $2\pi/40, u$ | 4.81E-04 | 2.00 | 1.84E-03 | 1.99 | 6.08E-06 | 3.00 | 2.90E-05 | 2.99 |
| $2\pi/40, q$ | 4.81E-04 | 2.00 | 1.84E-03 | 1.99 | 6.08E-06 | 3.00 | 2.90E-05 | 2.99 |
| $2\pi/80, u$ | 1.20E-04 | 2.00 | 4.62E-04 | 2.00 | 7.60E-07 | 3.00 | 3.63E-06 | 3.00 |
| $2\pi/80, q$ | 1.20E-04 | 2.00 | 4.62E-04 | 2.00 | 7.60E-07 | 3.00 | 3.63E-06 | 3.00 |
| $2\pi/160, u$ | 3.00E-05 | 2.00 | 1.15E-04 | 2.00 | 9.50E-08 | 3.00 | 4.53E-07 | 3.00 |
| $2\pi/160, q$ | 3.00E-05 | 2.00 | 1.15E-04 | 2.00 | 9.50E-08 | 3.00 | 4.53E-07 | 3.00 |

The conclusions are valid for general nonlinear multi-dimensional convection diffusion equations

$$u_t + \sum_{i=1}^d f_i(u)_{x_i} - \sum_{i=1}^d \sum_{j=1}^d (a_{ij}(u)u_{x_j})_{x_i} = 0, \quad (6)$$

where $a_{ij}(u)$ are entries of a symmetric and semi-positive definite matrix,
[Cockburn and Shu, SINUM 98; Xu and Shu, CMAME 07; Shu, Birkhäuser 09.](#)

Let us look at the one-dimensional nonlinear convection-diffusion equations

$$u_t + f(u)_x = (a(u)u_x)_x \quad (7)$$

with $a(u) \geq 0$. We again rewrite this equation as the following system

$$u_t + f(u)_x - (b(u)q)_x = 0, \quad q - B(u)_x = 0, \quad (8)$$

where

$$b(u) = \sqrt{a(u)}, \quad B(u) = \int^u b(u)du. \quad (9)$$

The semi-discrete LDG scheme is defined as follows. Find $u_h, q_h \in V_h^k$ such that, for all test functions $v_h, p_h \in V_h^k$ and all $1 \leq i \leq N$, we have

$$\begin{aligned} & \int_{I_j} (u_h)_t v_h dx - \int_{I_j} (f(u_h) - b(u_h)q_h)(v_h)_x dx \\ & + (\hat{f} - \hat{b}\hat{q})_{j+\frac{1}{2}} (v_h)_{j+\frac{1}{2}}^- - (\hat{f} - \hat{b}\hat{q})_{j-\frac{1}{2}} (v_h)_{j-\frac{1}{2}}^+ = 0, \quad (10) \\ & \int_{I_j} q_h p_h dx + \int_{I_j} B(u_h)(p_h)_x dx - \hat{B}_{j+\frac{1}{2}} (p_h)_{j+\frac{1}{2}}^- + \hat{B}_{j-\frac{1}{2}} (p_h)_{j-\frac{1}{2}}^+ = 0. \end{aligned}$$

We can still use the so-called “alternating fluxes” discussed before for the linear heat equation, now defined as

$$\hat{b} = \frac{B(u_h^+) - B(u_h^-)}{u_h^+ - u_h^-}, \quad \hat{q} = q_h^+, \quad \hat{B} = B(u_h^-). \quad (11)$$

The important point is that \hat{q} and \hat{B} should be chosen from different directions. Thus, the choice

$$\hat{b} = \frac{B(u_h^+) - B(u_h^-)}{u_h^+ - u_h^-}, \quad \hat{q} = q_h^-, \quad \hat{B} = B(u_h^+)$$

is also fine.

Notice that, even for this fully nonlinear case, from the second equation in the scheme (10), we can still solve q_h explicitly and locally (in cell I_j) in terms of u_h , by inverting the small mass matrix inside the cell I_j , thus justifying the terminology “local” discontinuous Galerkin methods.

It can be proved (Cockburn and Shu, SINUM 98) that, for the solution u_h , q_h to the semi-discrete LDG scheme (10), we still have the following “cell entropy inequality”

$$\frac{1}{2} \frac{d}{dt} \int_{I_j} (u_h)^2 dx + \int_{I_j} (q_h)^2 dx + \hat{F}_{j+\frac{1}{2}} - \hat{F}_{j-\frac{1}{2}} \leq 0 \quad (12)$$

for a consistent entropy flux

$$\hat{F}_{j+\frac{1}{2}} = \hat{F}(u_h(x_{j+\frac{1}{2}}^-, t), q_h(x_{j+\frac{1}{2}}^-, t); u_h(x_{j+\frac{1}{2}}^+, t), q_h(x_{j+\frac{1}{2}}^+))$$

satisfying $\hat{F}(u, q; u, q) = F(u) - ub(u)q$ where, as before,
 $F(u) = \int^u u f'(u) du$.

This, together with periodic or compactly supported boundary conditions, implies the following L^2 stability

$$\frac{d}{dt} \int_a^b (u_h)^2 dx + 2 \int_a^b (q_h)^2 dx \leq 0, \quad (13)$$

or

$$\|u_h(\cdot, t)\|^2 + 2 \int_0^t \|q_h(\cdot, \tau)\|^2 d\tau \leq \|u_h(\cdot, 0)\|^2. \quad (14)$$

A priori L^2 error estimates for smooth solutions are provided in Xu and Shu, CMAME 07.

Other DG methods for diffusion equations

Internal penalty DG methods

We still look at the heat equation

$$u_t = u_{xx}$$

multiplying by a test function v and integrating by parts, we obtain the equality

$$\int_{I_j} u_t v dx = - \int_{I_j} u_x v_x dx + (u_x)_{j+\frac{1}{2}} v_{j+\frac{1}{2}}^- - (u_x)_{j-\frac{1}{2}} v_{j-\frac{1}{2}}^+ \quad (15)$$

Summing over j , we obtain (with periodic boundary conditions)

$$\int_a^b u_t v dx = - \sum_{j=1}^N \int_{I_j} u_x v_x dx - \sum_{j=1}^N (u_x)_{j+\frac{1}{2}} [v]_{j+\frac{1}{2}} \quad (16)$$

where $[w] \equiv w^+ - w^-$. If we attempt to convert the equality (16) into a numerical scheme, we could try the following. Find $u_h \in V_h^k$ such that, for all test functions $v_h \in V_h^k$, we have

$$\int_a^b (u_h)_t (v_h) dx = - \sum_{j=1}^N \int_{I_j} (u_h)_x (v_h)_x dx - \sum_{j=1}^N \{(u_h)_x\}_{j+\frac{1}{2}} [v_h]_{j+\frac{1}{2}} \quad (17)$$

where $\{w\} \equiv \frac{1}{2}(w^+ + w^-)$. This scheme is actually exactly the same as the “bad scheme” we have shown before, which is known to be unstable as mentioned above.

Notice that the right-hand-side of (17) is not symmetric with respect to u_h and v_h . We can therefore add another term to symmetrize it, obtaining the following scheme. Find $u_h \in V_h^k$ such that, for all test functions $v_h \in V_h^k$, we have

$$\begin{aligned} \int_a^b (u_h)_t(v_h) dx &= - \sum_{j=1}^N \int_{I_j} (u_h)_x(v_h)_x dx \\ &\quad - \sum_{j=1}^N \{(u_h)_x\}_{j+\frac{1}{2}} [v_h]_{j+\frac{1}{2}} - \sum_{j=1}^N \{(v_h)_x\}_{j+\frac{1}{2}} [u_h]_{j+\frac{1}{2}}. \end{aligned} \quad (18)$$

Notice that, since the exact solution is continuous, the additional term $- \sum_{j=1}^N \{(v_h)_x\}_{j+\frac{1}{2}} [u_h]_{j+\frac{1}{2}}$ is zero if the numerical solution u_h is replaced by the exact solution u , hence the scheme is consistent.

Scheme (18) is symmetric, unfortunately it is still unconditionally unstable. In order to stabilize the scheme, a further penalty term must be added, resulting in the following symmetric internal penalty discontinuous Galerkin (SIPG) method (Wheeler, SINUM 78; Arnold, SINUM 82)

$$\begin{aligned}
 \int_a^b (u_h)_t(v_h) dx &= - \sum_{j=1}^N \int_{I_j} (u_h)_x(v_h)_x dx - \sum_{j=1}^N \{(u_h)_x\}_{j+\frac{1}{2}} [v_h]_{j+\frac{1}{2}} \\
 &\quad - \sum_{j=1}^N \{(v_h)_x\}_{j+\frac{1}{2}} [u_h]_{j+\frac{1}{2}} - \sum_{j=1}^N \frac{\alpha}{h} [u_h]_{j+\frac{1}{2}} [v_h]_{j+\frac{1}{2}}. \tag{19}
 \end{aligned}$$

Clearly, the scheme (19) is still symmetric, and it can be proved that, for sufficiently large α , it is stable and has optimal $O(h^{k+1})$ order convergence in L^2 .

The disadvantage of this scheme is that it involves a parameter α which has to be chosen adequately to ensure stability. Another possible way to obtain a stable scheme is to change the sign of the last term in the unstable scheme (18), resulting in the following non-symmetric internal penalty discontinuous Galerkin (NIPG) method (Baumann and Oden, CMAME 99; Oden, Babuska and Baumann, JCP 98)

$$\int_a^b (u_h)_t(v_h)dx = - \sum_{j=1}^N \int_{I_j} (u_h)_x(v_h)_x dx \\ - \sum_{j=1}^N \{(u_h)_x\}_{j+\frac{1}{2}} [v_h]_{j+\frac{1}{2}} + \sum_{j=1}^N \{(v_h)_x\}_{j+\frac{1}{2}} [u_h]_{j+\frac{1}{2}}. \quad (20)$$

This scheme is not symmetric, however it is L^2 stable and convergent, although it has a sub-optimal $O(h^k)$ order of L^2 errors for even k .

There are other types of DG methods involving the internal penalty methodology, for example the direct discontinuous Galerkin (DDG) methods of Liu and Yan (SINUM 09, CiCP 10).

Ultra weak discontinuous Galerkin methods

Ultra weak discontinuous Galerkin methods are designed in Cheng and Shu, Math Comp 08.

Let us again use the simple heat equation. If we multiply both sides by a test function v and integrate by parts twice, we obtain the equality

$$\begin{aligned} \int_{I_j} u_t v dx &= \int_{I_j} uv_{xx} dx + (u_x)_{j+\frac{1}{2}} v_{j+\frac{1}{2}} - (u_x)_{j-\frac{1}{2}} v_{j-\frac{1}{2}} \\ &\quad - u_{j+\frac{1}{2}} (v_x)_{j+\frac{1}{2}} + u_{j-\frac{1}{2}} (v_x)_{j-\frac{1}{2}}. \end{aligned} \quad (21)$$

We can then follow the general principle of designing DG schemes, namely converting the solution u and its derivatives at the cell boundary into numerical fluxes, and taking values of the test function v and its derivatives at the cell boundary by values inside the cell I_j , to obtain the following scheme. Find $u_h \in V_h^k$ such that, for all test functions $v_h \in V_h^k$ and all $1 \leq j \leq N$, we have

$$\begin{aligned} \int_{I_j} (u_h)_t v_h dx &= \int_{I_j} u_h (v_h)_{xx} dx + \hat{u}_{xj+\frac{1}{2}}^- (v_h)_{j+\frac{1}{2}}^- - \hat{u}_{xj-\frac{1}{2}}^+ (v_h)_{j-\frac{1}{2}}^+ \\ &\quad - \hat{u}_{j+\frac{1}{2}}^- ((v_h)_x)_{j+\frac{1}{2}}^- + \hat{u}_{j-\frac{1}{2}}^+ ((v_h)_x)_{j-\frac{1}{2}}^+. \end{aligned} \tag{22}$$

The crucial ingredient for the stability of the scheme (22) is still the choice of numerical fluxes. It is proved in Cheng and Shu, Math Comp 08 that the following choice of numerical fluxes

$$\hat{u}_{j+\frac{1}{2}} = (u_h)^{-}_{j+\frac{1}{2}}, \quad \hat{u}_{xj+\frac{1}{2}} = ((u_h)_x)^{+}_{j+\frac{1}{2}} + \frac{\alpha}{h} [u_h]_{j+\frac{1}{2}} \quad (23)$$

would yield a stable DG scheme if the constant $\alpha > 0$ is sufficiently large. Notice that the choice in (23) is a combination of alternating fluxes and internal penalty. The following choice of alternating fluxes would also work

$$\hat{u}_{j+\frac{1}{2}} = (u_h)^{+}_{j+\frac{1}{2}}, \quad \hat{u}_{xj+\frac{1}{2}} = ((u_h)_x)^{-}_{j+\frac{1}{2}} + \frac{\alpha}{h} [u_h]_{j+\frac{1}{2}}.$$

In numerical experiments, optimal L^2 convergence rate of $O(h^{k+1})$ is observed for all $k \geq 1$. The scheme can be easily generalized to the general nonlinear convection-diffusion equations with the same stability property.

LDG method for KdV equations

Now, the Korteweg-de Vries (KdV) equation:

$$u_t + (\alpha u + \beta u^2)_x + \sigma u_{xxx} = 0$$

More generally, in 1D:

$$u_t + f(u)_x + (r'(u)g(r(u)_x)_x)_x = 0$$

and in multi dimensions:

$$u_t + \sum_{i=1}^d f_i(u)_{x_i} + \sum_{i=1}^d \left(r'_i(u) \sum_{j=1}^d g_{ij}(r_i(u)_{x_i})_{x_j} \right)_{x_i} = 0$$

A “preview”: simple equation

$$u_t + u_{xxx} = 0$$

Again rewrite into a first order system

$$u_t + p_x = 0, \quad p - q_x = 0, \quad q - u_x = 0.$$

Then again *formally* use the DG method: find $u, p, q \in V_h$ such that, for all test functions $v, w, z \in V_h$,

$$\int_{I_j} u_t v dx - \int_{I_j} p v_x dx + \hat{p}_{j+\frac{1}{2}} v_{j+\frac{1}{2}}^- - \hat{p}_{j-\frac{1}{2}} v_{j-\frac{1}{2}}^+ = 0,$$

$$\int_{I_j} p w dx + \int_{I_j} q w_x dx - \hat{q}_{j+\frac{1}{2}} w_{j+\frac{1}{2}}^- + \hat{q}_{j-\frac{1}{2}} w_{j-\frac{1}{2}}^+ = 0,$$

$$\int_{I_j} q z dx + \int_{I_j} u z_x dx - \hat{u}_{j+\frac{1}{2}} z_{j+\frac{1}{2}}^- + \hat{u}_{j-\frac{1}{2}} z_{j-\frac{1}{2}}^+ = 0.$$

Again, a key ingredient of the design of the LDG method is the choice of the numerical fluxes \hat{u} , \hat{q} and \hat{p} (now, upwinding principle partially available, after all, the solution with the initial condition $\sin(x)$ is $\sin(x + t)$, hence the wind blows from right to left).

The following choice of **alternating** + **upwinding**

$$\hat{p}_{j+\frac{1}{2}} = p_{j+\frac{1}{2}}^+, \quad \hat{q}_{j+\frac{1}{2}} = q_{j+\frac{1}{2}}^+, \quad \hat{u}_{j+\frac{1}{2}} = u_{j+\frac{1}{2}}^-,$$

would guarantee stability. The choice is not unique:

$$\hat{p}_{j+\frac{1}{2}} = p_{j+\frac{1}{2}}^-, \quad \hat{q}_{j+\frac{1}{2}} = q_{j+\frac{1}{2}}^+, \quad \hat{u}_{j+\frac{1}{2}} = u_{j+\frac{1}{2}}^+,$$

would also work.

Table 3: $u_t + u_{xxx} = 0$. $u(x, 0) = \sin(x)$.

| k | | N=10 | N=20 | | N=40 | | N=80 | |
|---|------------|------------|------------|-------|------------|-------|------------|-------|
| | | error | error | order | error | order | error | order |
| 0 | L^2 | 2.2534E-01 | 1.2042E-01 | 0.91 | 6.2185E-02 | 0.95 | 3.1582E-02 | 0.98 |
| | L^∞ | 4.3137E-01 | 2.1977E-01 | 0.97 | 1.1082E-01 | 0.98 | 5.5376E-02 | 0.99 |
| 1 | L^2 | 1.7150E-02 | 4.2865E-03 | 2.00 | 1.0716E-03 | 2.00 | 2.6792E-04 | 2.00 |
| | L^∞ | 5.8467E-02 | 1.5757E-02 | 1.89 | 4.0487E-03 | 1.96 | 1.0210E-03 | 1.99 |
| 2 | L^2 | 8.5803E-04 | 1.0823E-04 | 2.98 | 1.3559E-05 | 2.99 | 1.6958E-06 | 3.00 |
| | L^∞ | 4.0673E-03 | 5.1029E-04 | 2.99 | 6.4490E-05 | 2.98 | 8.0722E-06 | 3.00 |
| 3 | L^2 | 3.3463E-05 | 2.1035E-06 | 3.99 | 1.3166E-07 | 3.99 | 8.2365E-09 | 3.99 |
| | L^∞ | 1.8185E-04 | 1.1157E-05 | 3.97 | 7.2362E-07 | 3.99 | 4.5593E-08 | 3.99 |

Optimal in L^2 error estimates for not only u but also its derivatives can be proved. Xu and Shu, SINUM 2012.

The scheme can be designed for the general nonlinear case along the same lines.

For the general multi-dimensional nonlinear case

$$u_t + \sum_{i=1}^d f_i(u)_{x_i} + \sum_{i=1}^d \left(r'_i(u) \sum_{j=1}^d g_{ij}(r_i(u)_{x_i})_{x_j} \right)_{x_i} = 0$$

We can prove cell entropy inequality and L^2 stability. Yan and Shu, SINUM 02.

For the two dimensional KdV equation

$$u_t + f(u)_x + g(u)_y + u_{xxx} + u_{yyy} = 0,$$

and the Zakharov-Kuznetsov (ZK) equation

$$u_t + (3u^2)_x + u_{xxx} + u_{xyy} = 0,$$

We can prove error estimates of $O(h^{k+1/2})$ in L^2 for P^k elements in 1D and for Q^k elements in 2D, and of $O(h^k)$ for P^k elements in 2D. [Yan and Shu, SINUM 02 \(1D linear\)](#) and [Xu and Shu, CMAME 07](#).

Numerical example: zero dispersion limit of conservation laws.

Solutions of the KdV equation with small dispersion coefficient

$$u_t + \left(\frac{u^2}{2} \right)_x + \epsilon u_{xxx} = 0. \quad (24)$$

with an initial condition

$$u(x, 0) = 2 + 0.5 \sin(2\pi x) \quad (25)$$

for $x \in [0, 1]$ and periodic boundary conditions,

$$\epsilon = 10^{-4}, 10^{-5}, 10^{-6} \text{ and } 10^{-7}.$$

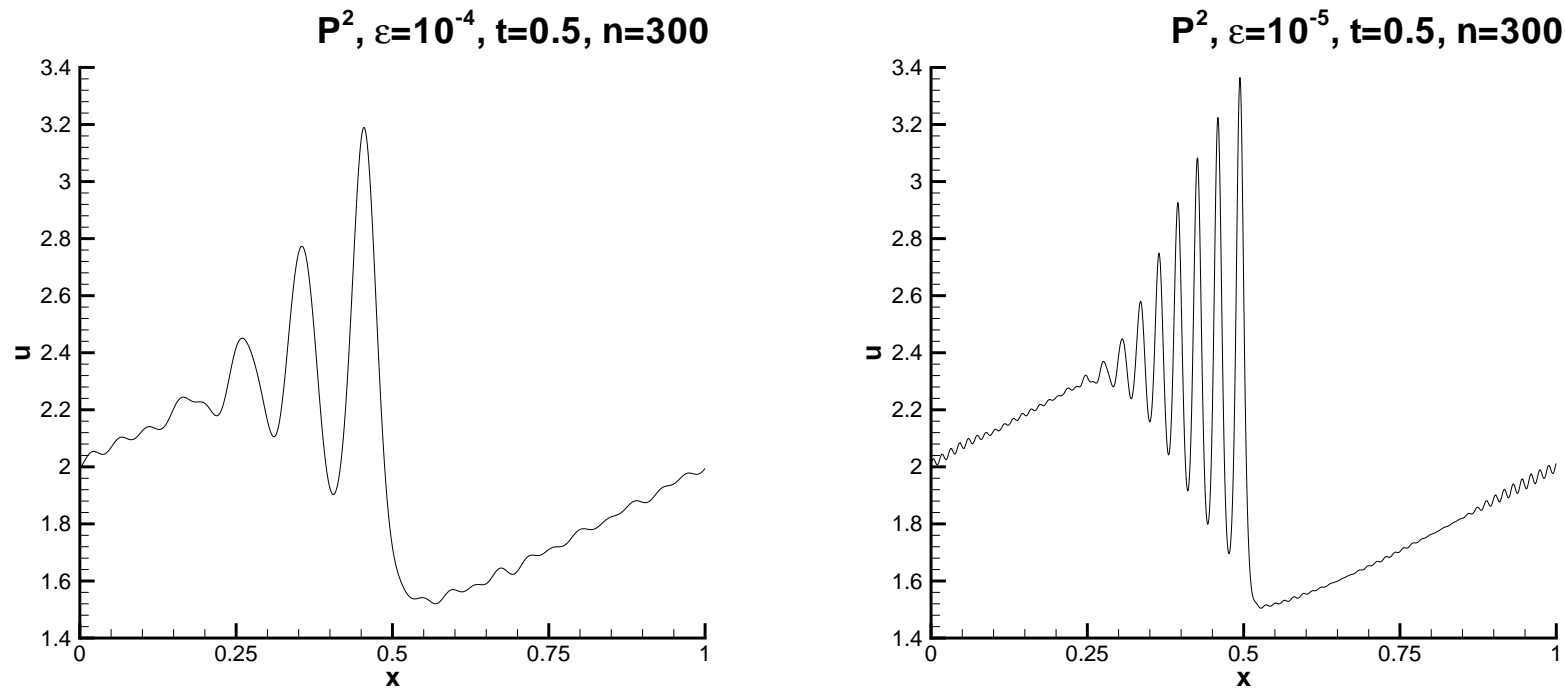


Figure 2: Zero dispersion limit of conservation laws. P^2 elements at $t = 0.5$. Left: $\epsilon = 10^{-4}$ with 300 cells; right: $\epsilon = 10^{-5}$ with 300 cells.

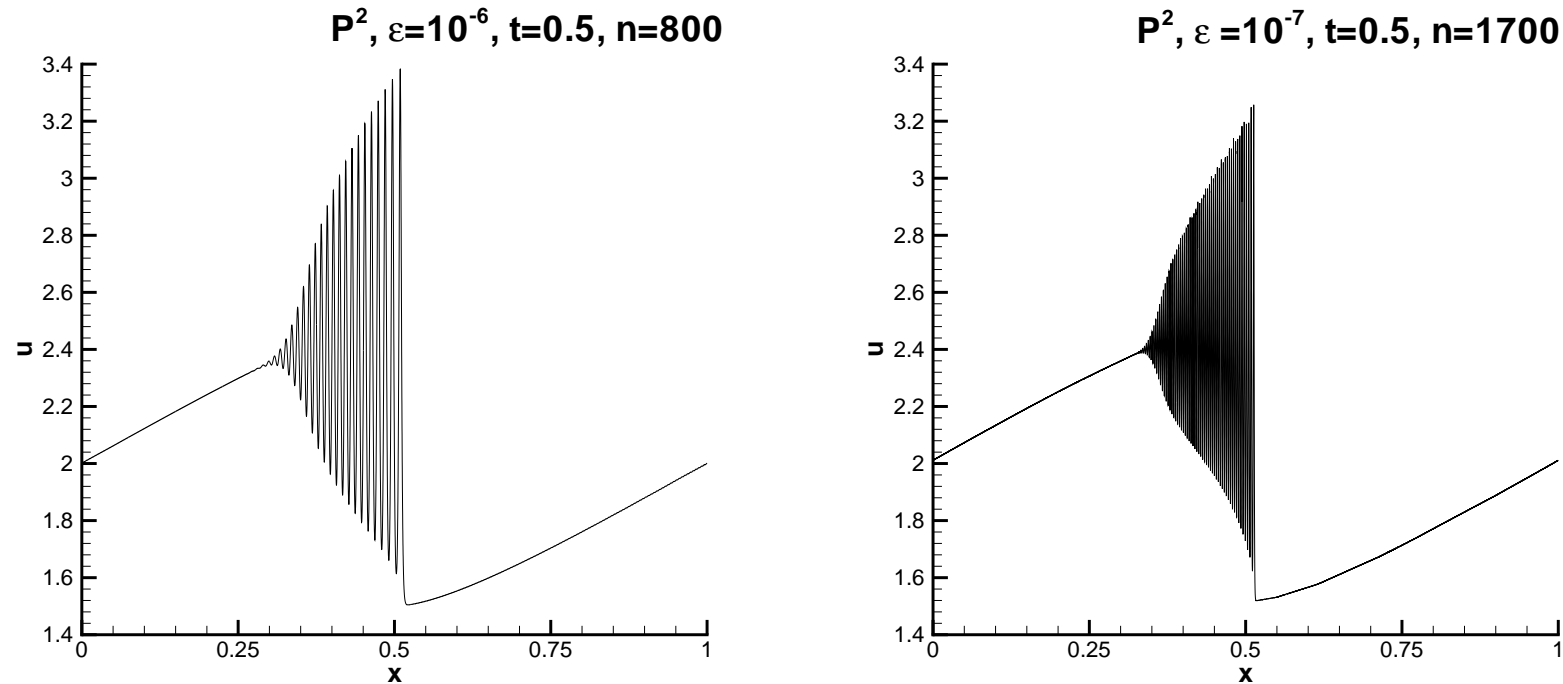


Figure 3: Zero dispersion limit of conservation laws. P^2 elements at $t = 0.5$. Left: $\epsilon = 10^{-6}$ with 800 cells; right: $\epsilon = 10^{-7}$ with 1700 cells.

LDG methods for other diffusive equations

LDG methods have been designed for the following diffusive equations:

(1) The bi-harmonic type equation

$$u_t + \sum_{i=1}^d f_i(u)_{x_i} + \sum_{i=1}^d (a_i(u_{x_i}) u_{x_i x_i})_{x_i x_i} = 0 \quad (26)$$

We can prove a cell entropy inequality and L^2 stability [Yan and Shu, JSC 02](#) for the general nonlinear problem and an optimal L^2 error estimates [Dong and Shu, SINUM 09](#) for the linear biharmonic and linearized Cahn-Hilliard equations.

Both the schemes and the analysis can be generalized to higher even order diffusive PDEs, e.g. the error estimate in [Dong and Shu, SINUM 09](#) is given also for higher even order linear diffusive PDEs.

(2) The Kuramoto-Sivashinsky type equations

$$u_t + f(u)_x - (a(u)u_x)_x + (r'(u)g(r(u)_x)_x)_x + (s(u_x)u_{xx})_{xx} = 0, \quad (27)$$

We prove a cell entropy inequality and L^2 stability in [Xu and Shu, CMAME 06.](#)

For the Kuramoto-Sivashinsky equation

$$u_t + uu_x + u_{xx} + u_{xxxx} = 0$$

we show the result of chaotic behavior.

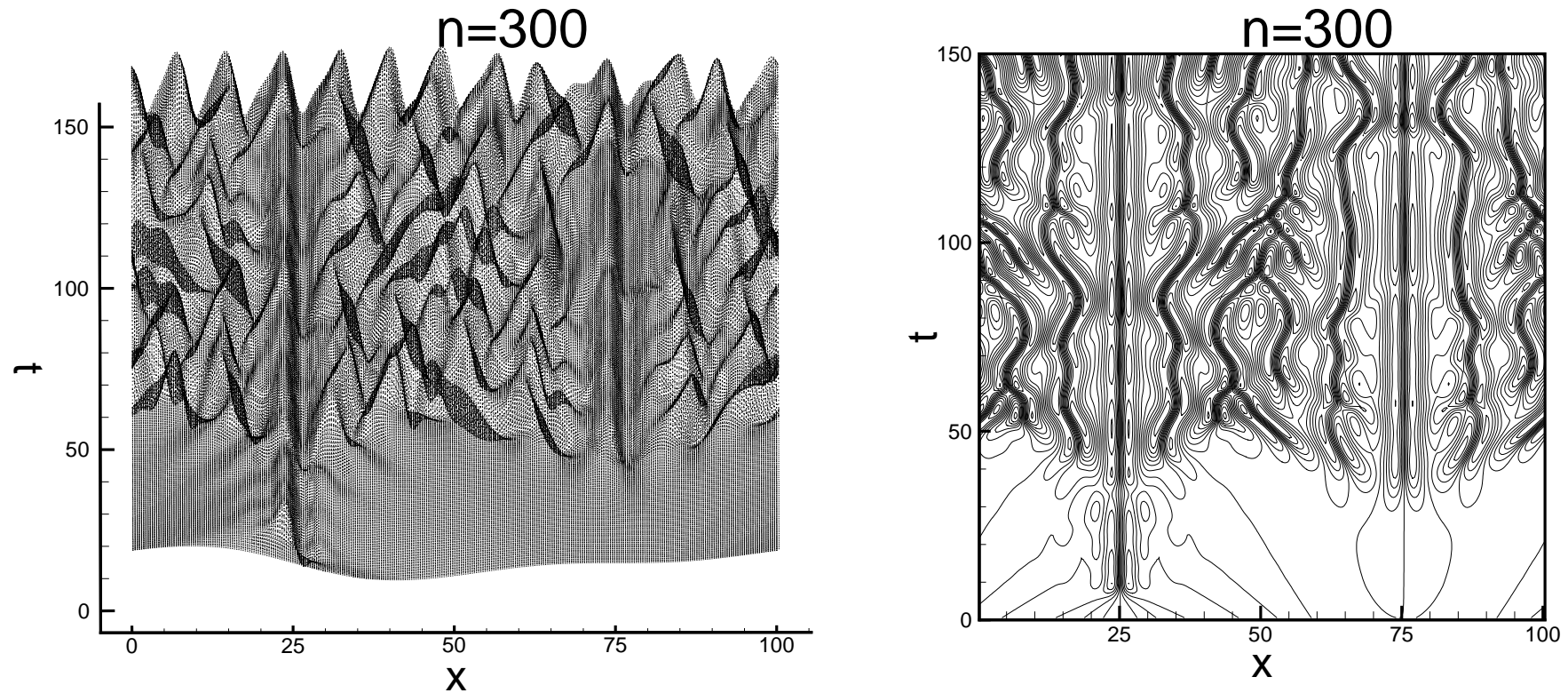


Figure 4: The chaotic solution of the Kuramoto-Sivashinsky equation. Periodic boundary condition in $[0, 32\pi]$, P^2 elements with $N = 300$ uniform cells.

(3) Device simulation models in semi-conductor device simulations: drift-diffusion, hydrodynamic, energy transport, high field, kinetic and Boltzmann-Poisson models, formulations of DG-LDG schemes and error estimates. [Liu and Shu, JCE 04; ANM 07; Sci in China 10; Cheng, Gamba, Majorana and Shu, JCE 08; CMAME 09.](#)

(4) Cahn-Hilliard equation

$$u_t = \nabla \cdot \left(b(u) \nabla (-\gamma \Delta u + \Psi'(u)) \right), \quad (28)$$

and the Cahn-Hilliard system

$$\mathbf{u}_t = \nabla \cdot (\mathbf{B}(\mathbf{u}) \nabla \omega), \quad \omega = -\gamma \Delta \mathbf{u} + D\Psi(\mathbf{u}), \quad (29)$$

where $\{D\Psi(\mathbf{u})\}_l = \frac{\partial \Psi(\mathbf{u})}{\partial u_l}$ and γ is a positive constant.

We design LDG methods and prove the energy stability for the general nonlinear case in [Xia, Xu and Shu, JCP 07; CiCP 09](#).

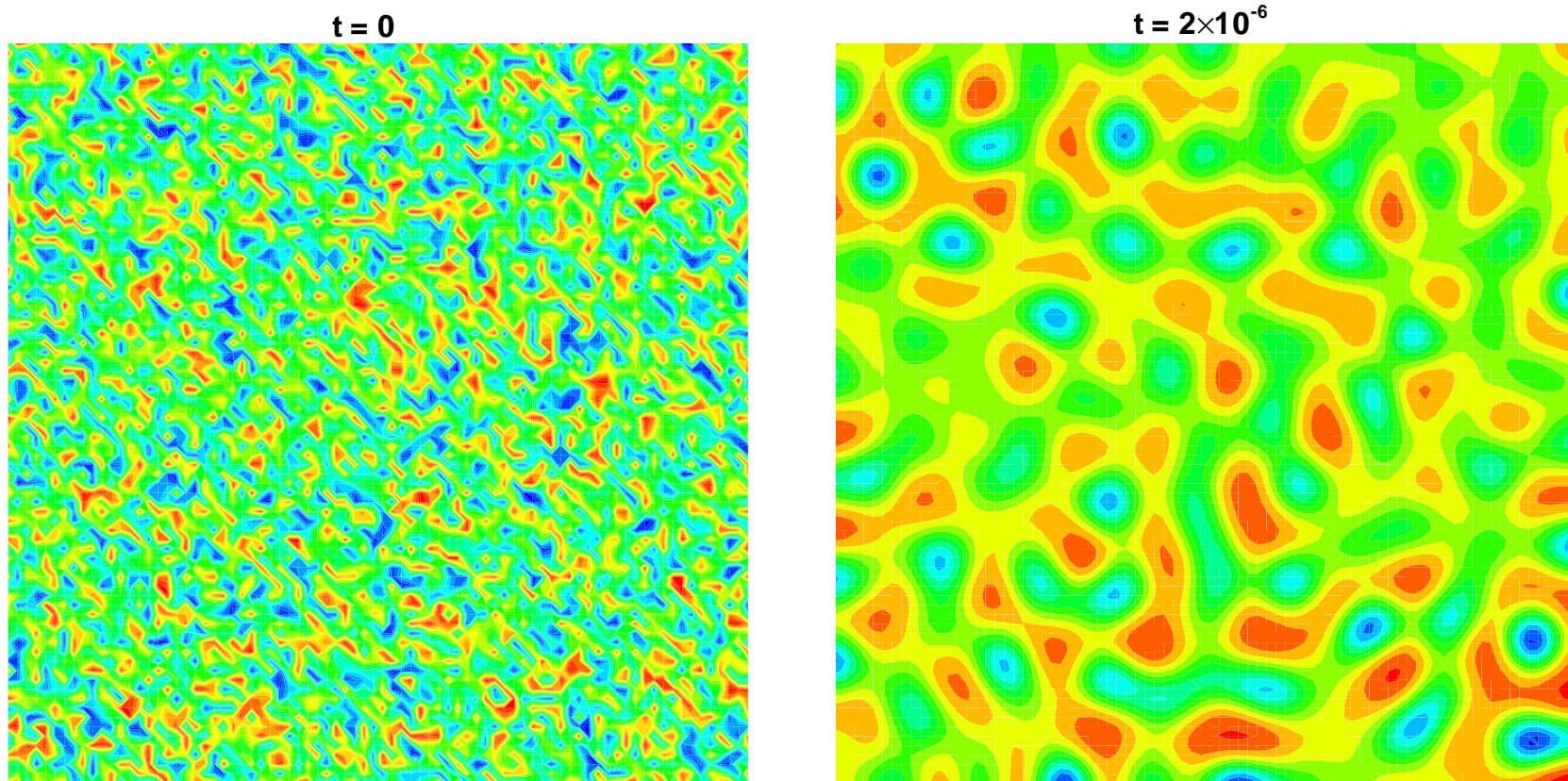


Figure 5: The contours evolution of $u(\mathbf{x}, t)$ for the Cahn-Hilliard equation at different time from a randomly perturbed initial condition with P^1 element on the uniform mesh with 80×80 cells.

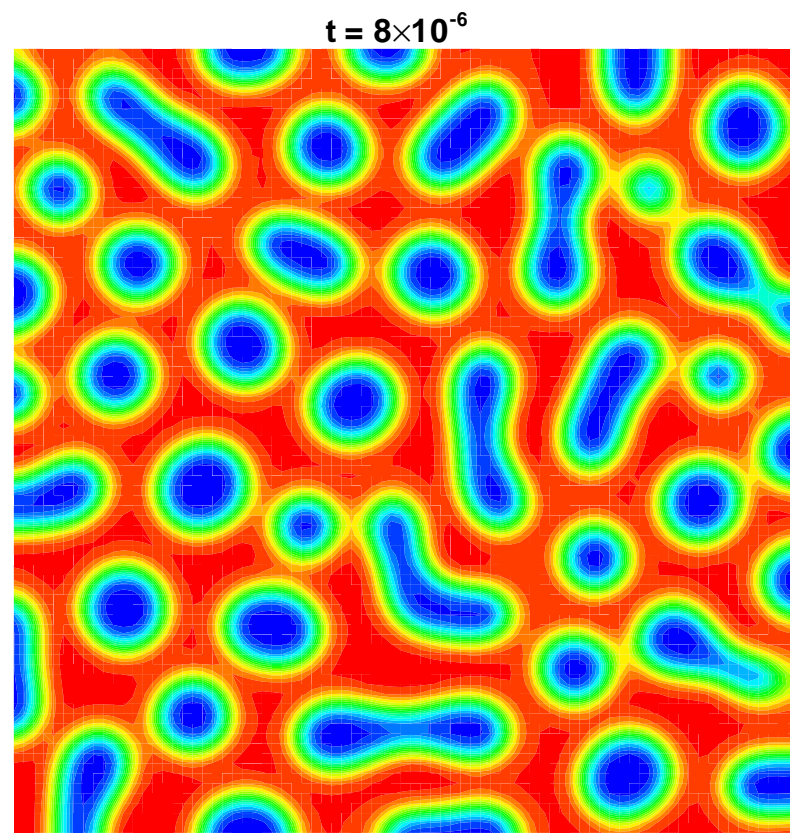
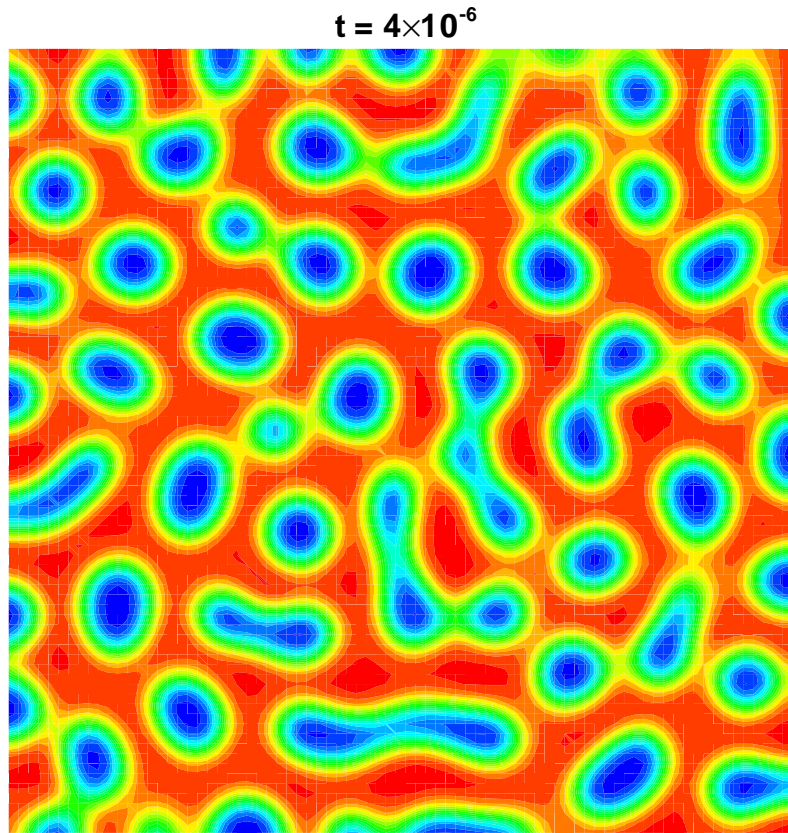


Figure 6: continued.

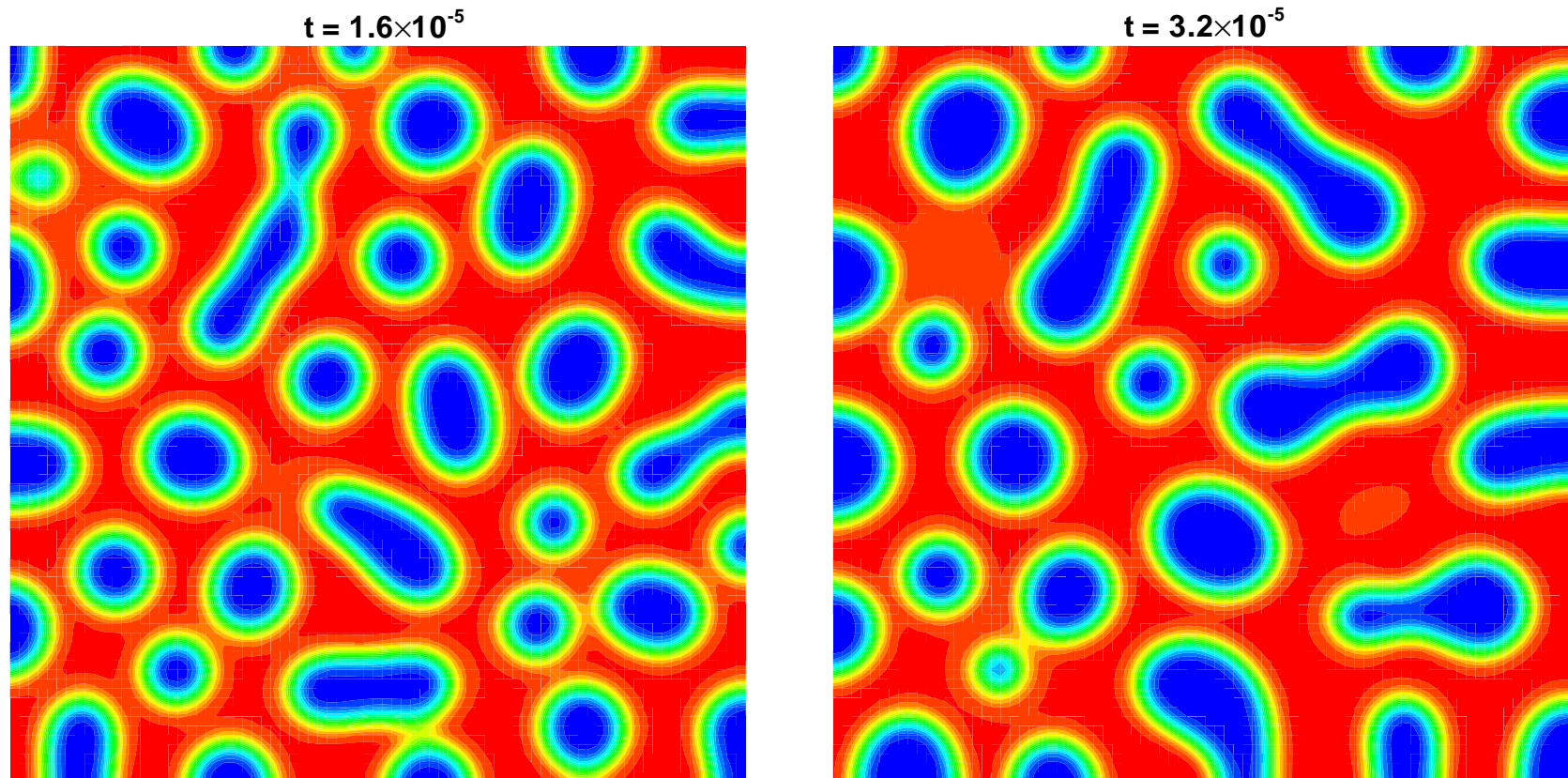


Figure 7: continued.

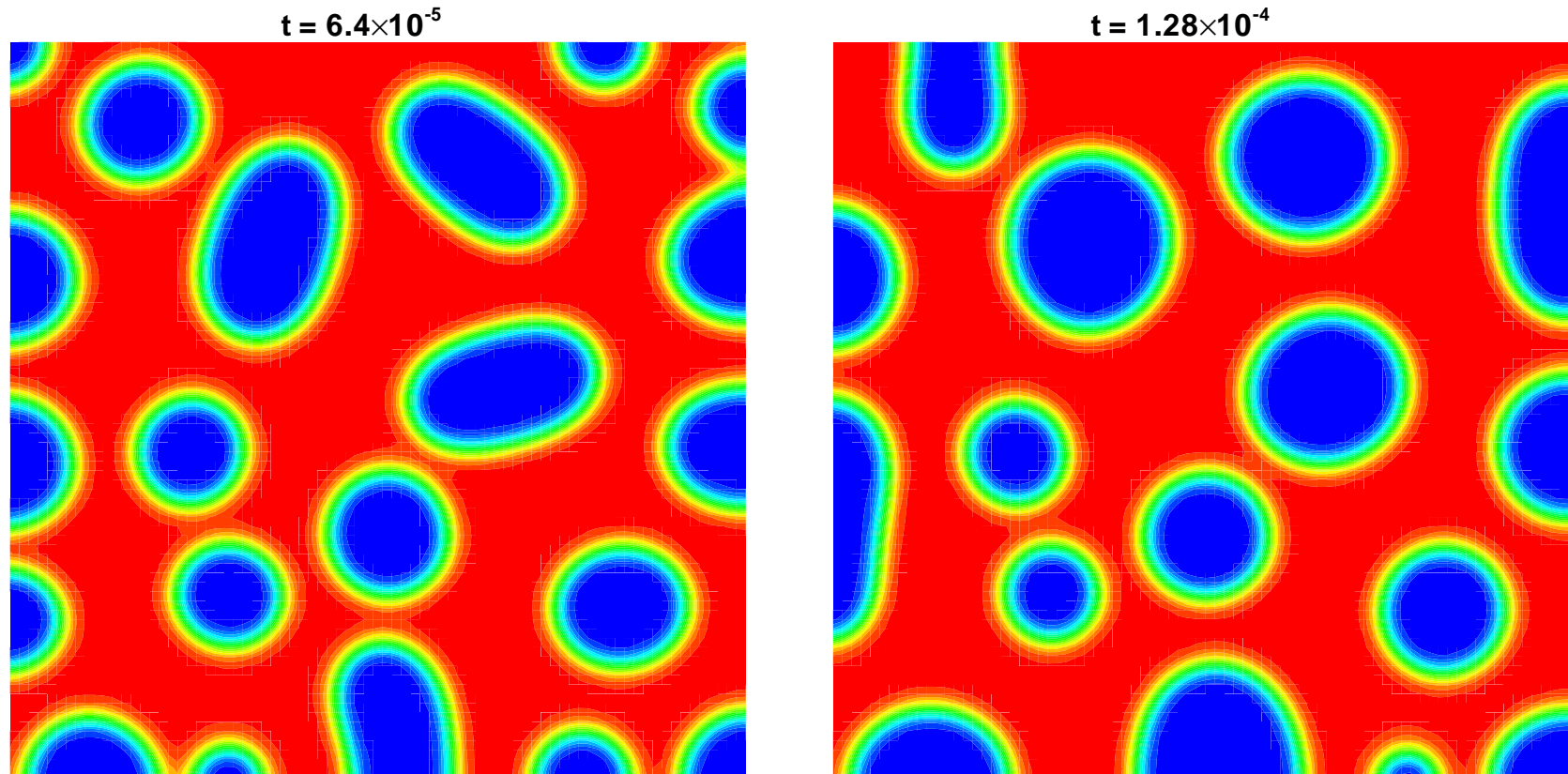


Figure 8: continued.

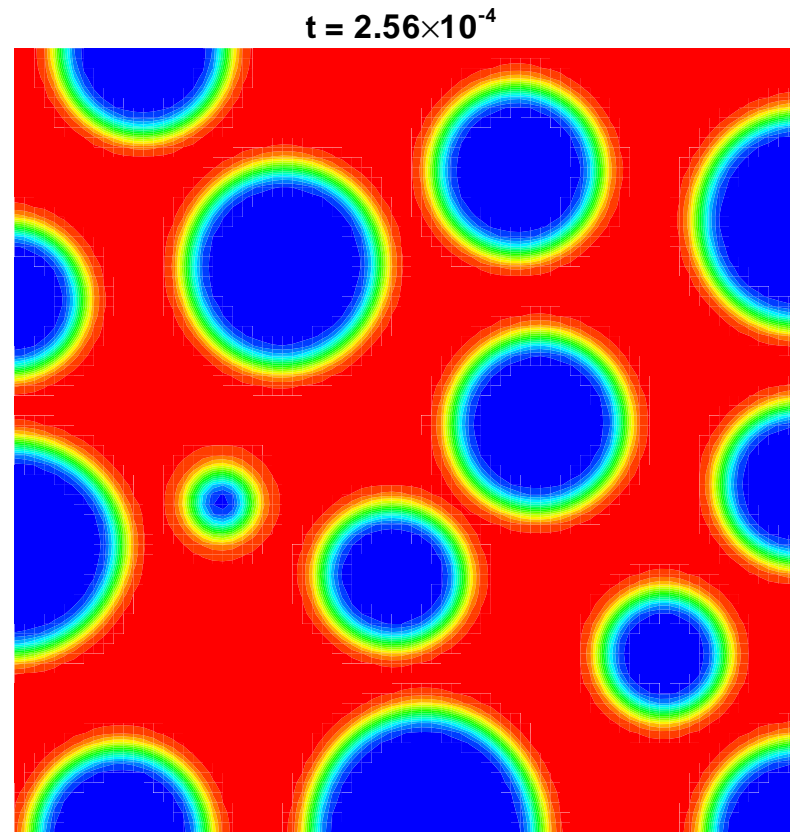


Figure 9: continued.

(5) The surface diffusion equation

$$u_t + \nabla \cdot \left(Q \left(\mathbf{I} - \frac{\nabla u \otimes \nabla u}{Q^2} \right) \nabla H \right) = 0 \quad (30)$$

where Q is the area element

$$Q = \sqrt{1 + |\nabla u|^2} \quad (31)$$

and H is the mean curvature of the domain boundary Γ

$$H = \nabla \cdot \left(\frac{\nabla u}{Q} \right) \quad (32)$$

and the Willmore flow

$$u_t + Q \nabla \cdot \left(\frac{1}{Q} \left(\mathbf{I} - \frac{\nabla u \otimes \nabla u}{Q^2} \right) \nabla (QH) \right) - \frac{1}{2} Q \nabla \cdot \left(\frac{H^2}{Q} \nabla u \right) = 0. \quad (33)$$

We develop LDG methods and prove their energy stability in [Xu and Shu, JSC 09.](#)

LDG methods for other dispersive wave equations

LDG methods have been designed for the following dispersive wave equations containing higher order (usually odd order) derivatives:

(1) The partial differential equations with five derivatives

$$U_t + \sum_{i=1}^d f_i(U)_{x_i} + \sum_{i=1}^d g_i(U_{x_i x_i})_{x_i x_i x_i} = 0 \quad (34)$$

We can prove a cell entropy inequality and L^2 stability, Yan and Shu, JSC 02.

(2) The $K(m, n)$ equation

$$u_t + (u^m)_x + (u^n)_{xxx} = 0,$$

with *compactons* solutions.

We obtain a L^{n+1} stable LDG scheme for the $K(n, n)$ equation with odd n , and a linearly stable LDG scheme for other cases, [Levy, Shu and Yan, JCP 04](#).

(3) The KdV-Burgers type (KdVB) equations

$$u_t + f(u)_x - (a(u)u_x)_x + (r'(u)g(r(u)_x)_x)_x = 0 \quad (35)$$

We prove a cell entropy inequality and L^2 stability, and obtain L^2 error estimate of $O(h^{k+1/2})$ for the linearized version in [Xu and Shu, JCM 04](#).

A special case is the KdV-Burgers equation

$$u_t + \varepsilon uu_x - \alpha u_{xx} + \beta u_{xxx} = 0$$

We fix $\varepsilon = 0.2$ and $\beta = 0.1$, then change α .

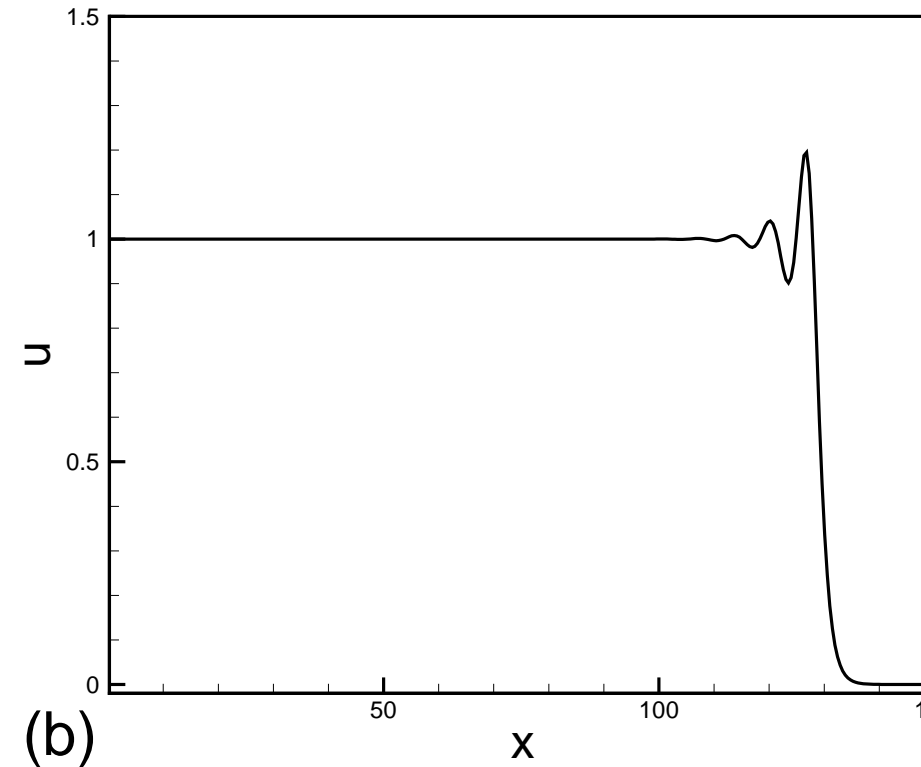
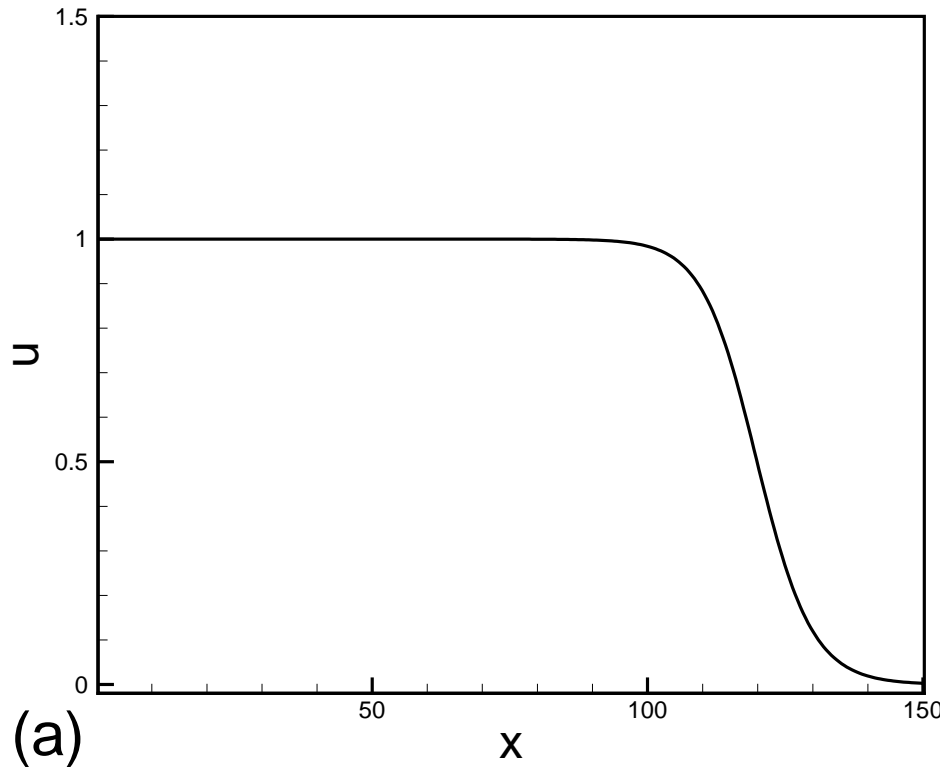


Figure 10: KdVB type solutions at time $t = 800$, $0 \leq x \leq 150$, $\varepsilon = 0.2$ and $\beta = 0.1$. P^1 elements with 320 cells. (a) $\alpha = 0.5$; (b) $\alpha = 0.05$.

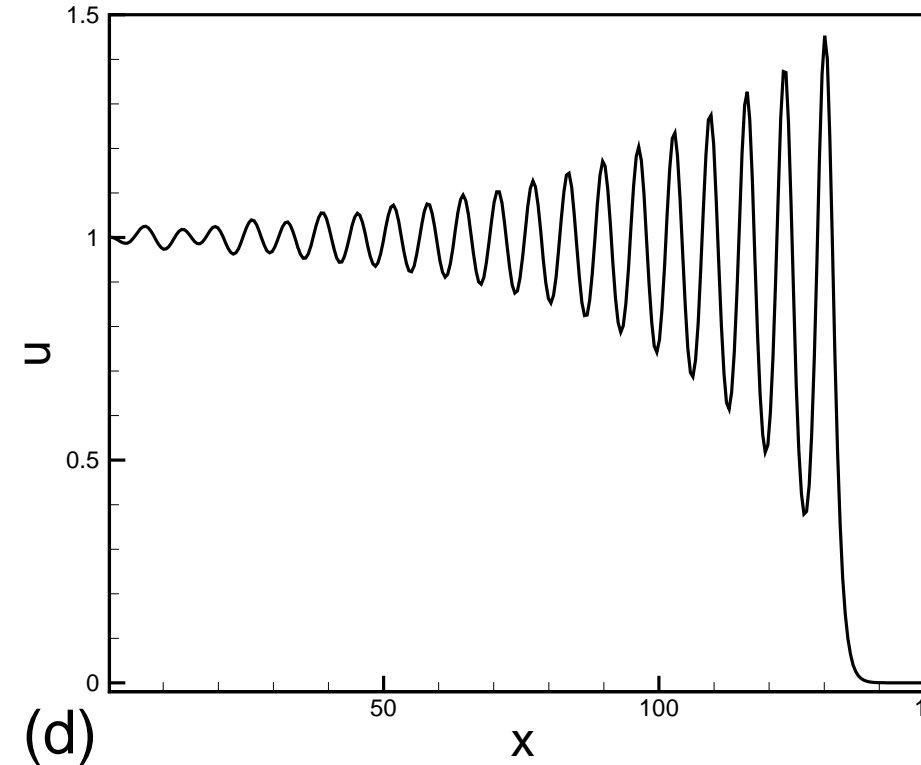
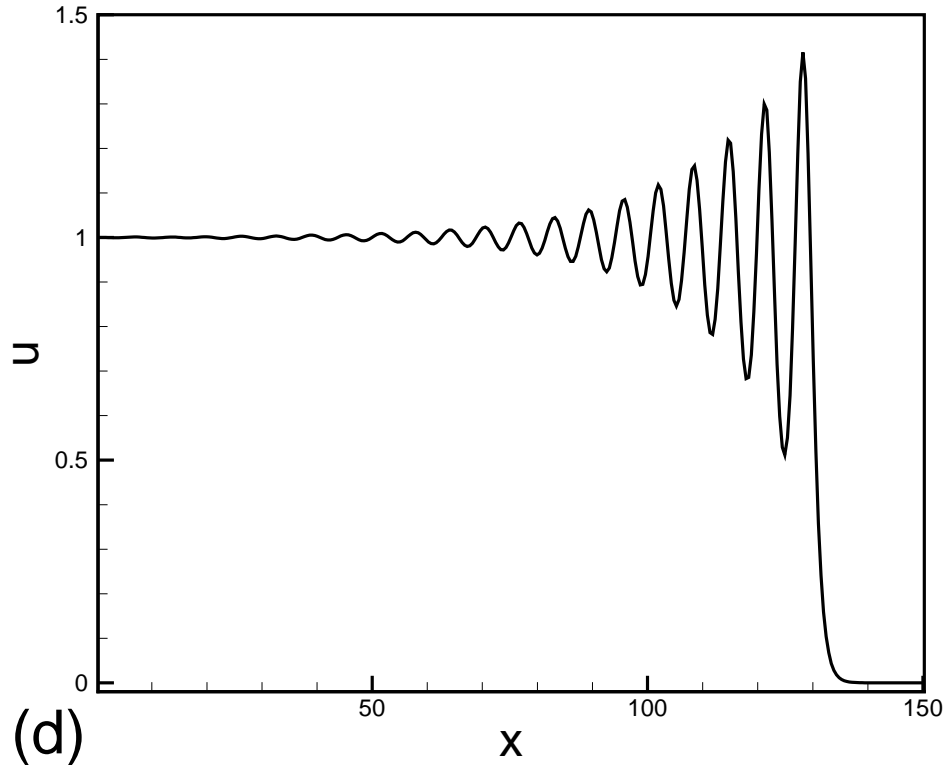


Figure 11: KdVB type solutions at time $t = 800$, $0 \leq x \leq 150$, $\varepsilon = 0.2$ and $\beta = 0.1$. P^1 elements with 320 cells. (c) $\alpha = 0.01$; (d) $\alpha = 0.005$.

(4) The fifth-order KdV type equations

$$u_t + f(u)_x + (r'(u)g(r(u)_x)_x)_x + (s'(u)h(s(u)_{xx})_{xx})_x = 0 \quad (36)$$

We prove a cell entropy inequality and L^2 stability in [Xu and Shu, JCM 04](#).

A special case is the Kawahara equation

$$u_t + uu_x + u_{xxx} - \delta u_{xxxxx} = 0$$

We show the result with the compact initial condition

$$u_0(x) = \begin{cases} A \cos^2(Bx - C) & |Bx - C| \leq \pi/2 \\ 0 & \text{otherwise} \end{cases}$$

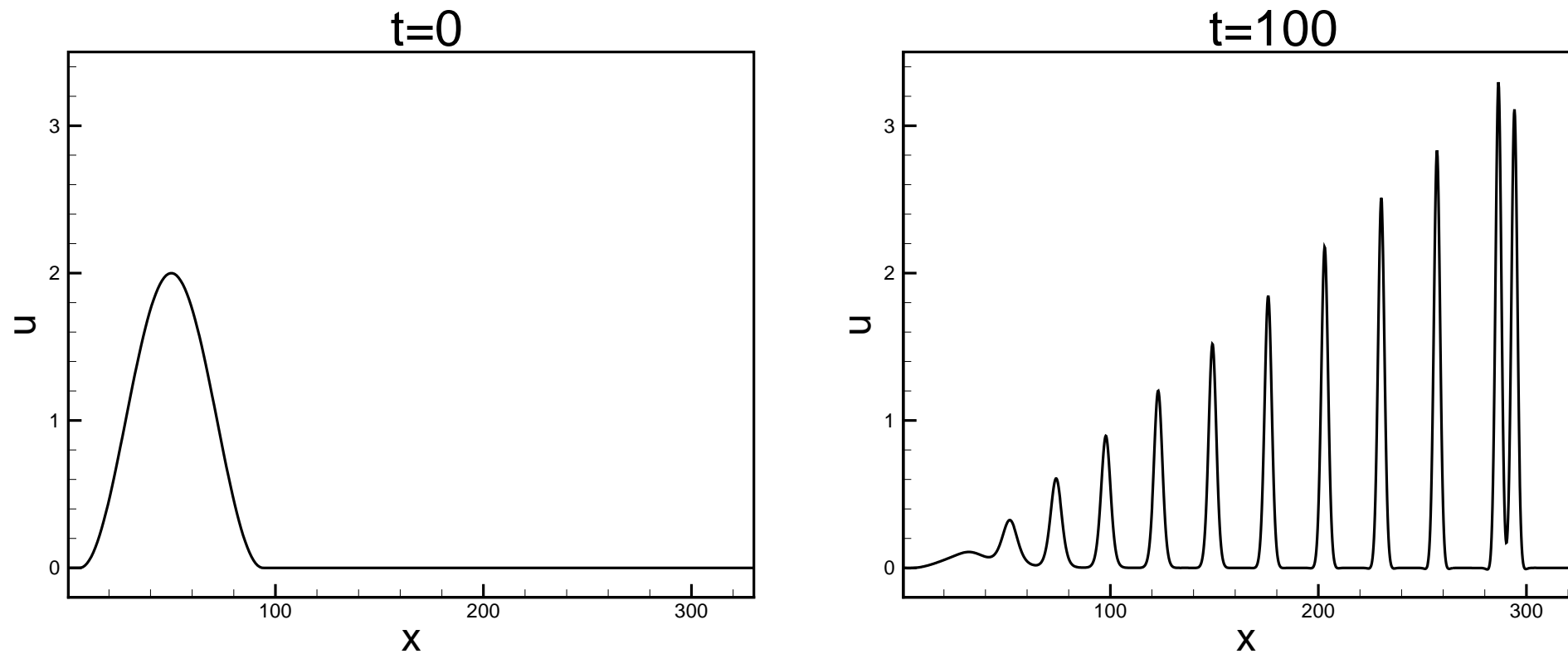


Figure 12: The pulsating multiplet solution for $\delta = 0.5$ in $[0, 330]$ using P^2 elements with 1500 cells, where $A = 2$, $B = 1/28$ and $C = 50/28$.

(5) The fifth-order fully nonlinear $K(n, n, n)$ equations

$$u_t + (u^n)_x + (u^n)_{xxx} + (u^n)_{xxxxx} = 0 \quad (37)$$

We prove L^{n+1} stability for odd n in [Xu and Shu, JCM 04](#).

(6) The generalized nonlinear Schrödinger (NLS) equation

$$i u_t + \Delta u + f(|u|^2)u = 0, \quad (38)$$

and the coupled nonlinear Schrödinger equation

$$\begin{cases} i u_t + i \alpha u_x + u_{xx} + \beta u + \kappa v + f(|u|^2, |v|^2)u = 0 \\ i v_t - i \alpha v_x + v_{xx} - \beta u + \kappa v + g(|u|^2, |v|^2)v = 0 \end{cases} \quad (39)$$

We prove a cell entropy inequality and L^2 stability, and obtain L^2 error estimate of $O(h^{k+1/2})$ for the linearized version in [Xu and Shu, JCP 05](#).

Singular solutions for the two-dimensional NLS equation

$$i u_t + u_{xx} + u_{yy} + |u|^2 u = 0$$

with the initial condition

$$u(x, y) = (1 + \sin x)(2 + \sin y)$$

and a periodic boundary condition. Strong evidence of a singularity in finite time is obtained, although there is no rigorous proof of breakdown in this case. The solution is computed with a periodic boundary condition in $[0, 2\pi]$ using P^2 elements with 120×120 uniform cells.

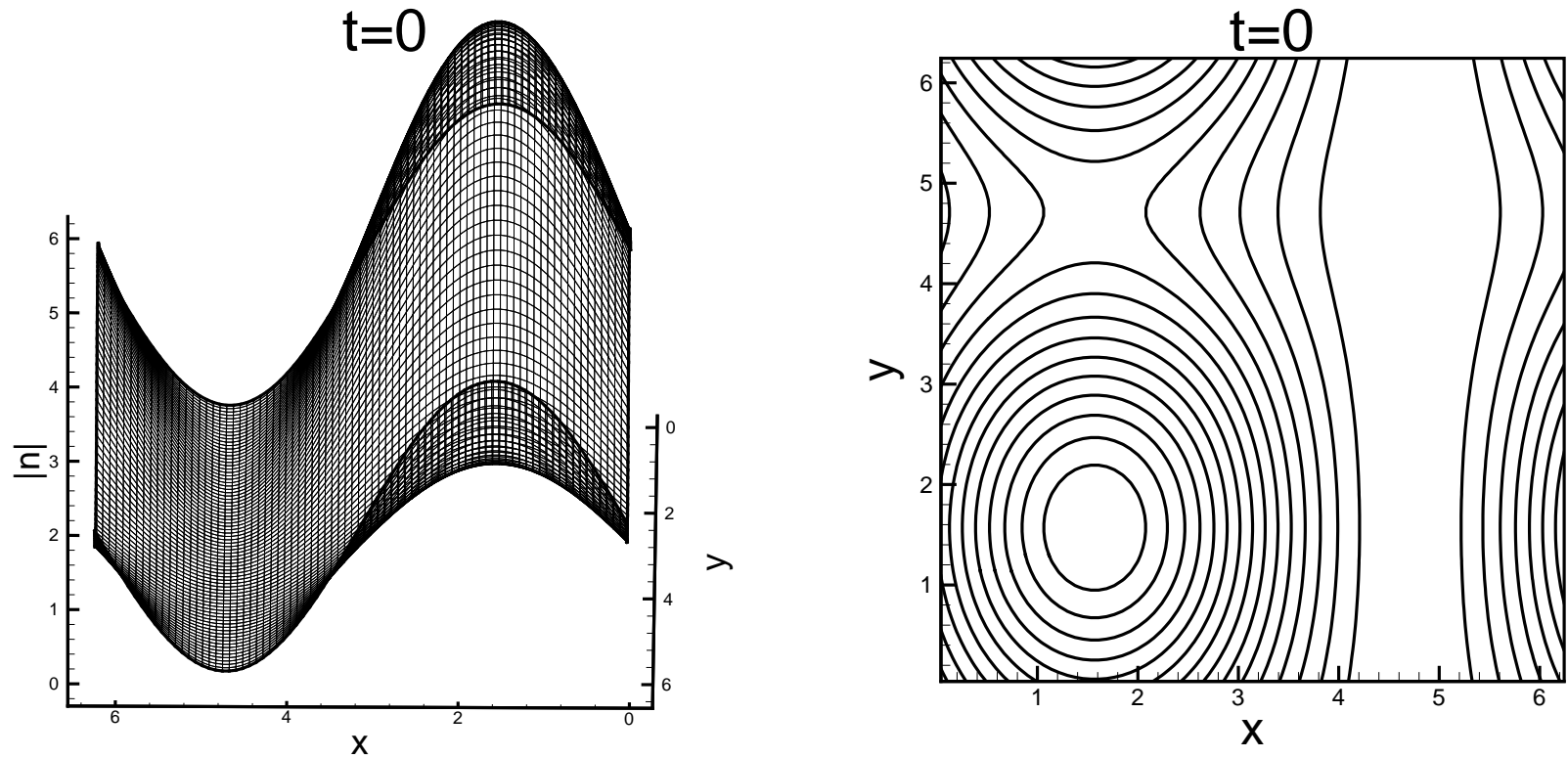


Figure 13: Initial condition.

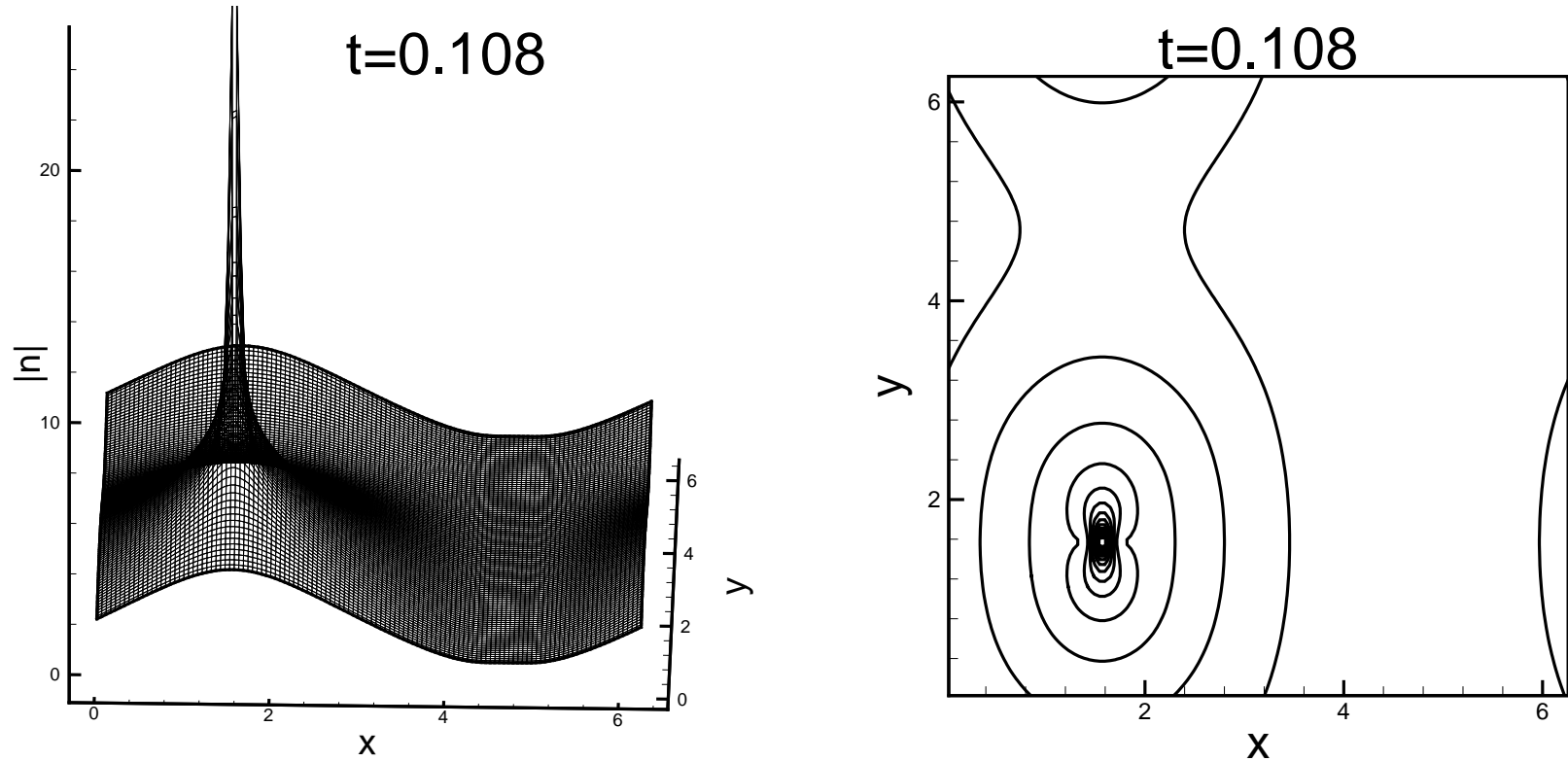


Figure 14: The singular solution of the two dimensional NLS equation. Periodic boundary condition in $[0, 2\pi]$. P^2 elements with 120×120 uniform cells.

(7) The Ito-type coupled KdV equations

$$u_t + \alpha uu_x + \beta vv_x + \gamma u_{xxx} = 0,$$

$$v_t + \beta(uv)_x = 0,$$

We prove a cell entropy inequality and L^2 stability in [Xu and Shu, CMAME 06.](#)

For the Ito's equation

$$u_t - (3u^2 + v^2)_x - u_{xxx} = 0,$$

$$v_t - 2(uv)_x = 0,$$

The result for u behaves like dispersive wave solutions and the result for v behaves like shock wave solutions.

(8) The Kadomtsev-Petviashvili (KP) equation

$$(u_t + 6uu_x + u_{xxx})_x + 3\sigma^2 u_{yy} = 0, \quad (40)$$

where $\sigma^2 = -1$ (KP-I) or $\sigma^2 = 1$ (KP-II).

This equation is equivalent to

$$u_t + 6(uu_x) + u_{xxx} + 3\sigma^2 \partial_x^{-1} u_{yy} = 0 \quad (41)$$

where the non-local operator ∂_x^{-1} makes the equation well-posed only in the restricted space

$$\mathcal{V}(R^2) = \left\{ f : \int_{R^2} \left(1 + \xi^2 + \frac{\eta^2}{\xi^2}\right) |\hat{f}(\xi, \eta)|^2 d\xi d\eta < \infty \right\}$$

Hence there is a technical difficulty in designing the LDG method.

We prove the L^2 stability in [Xu and Shu, Physica D 05](#).

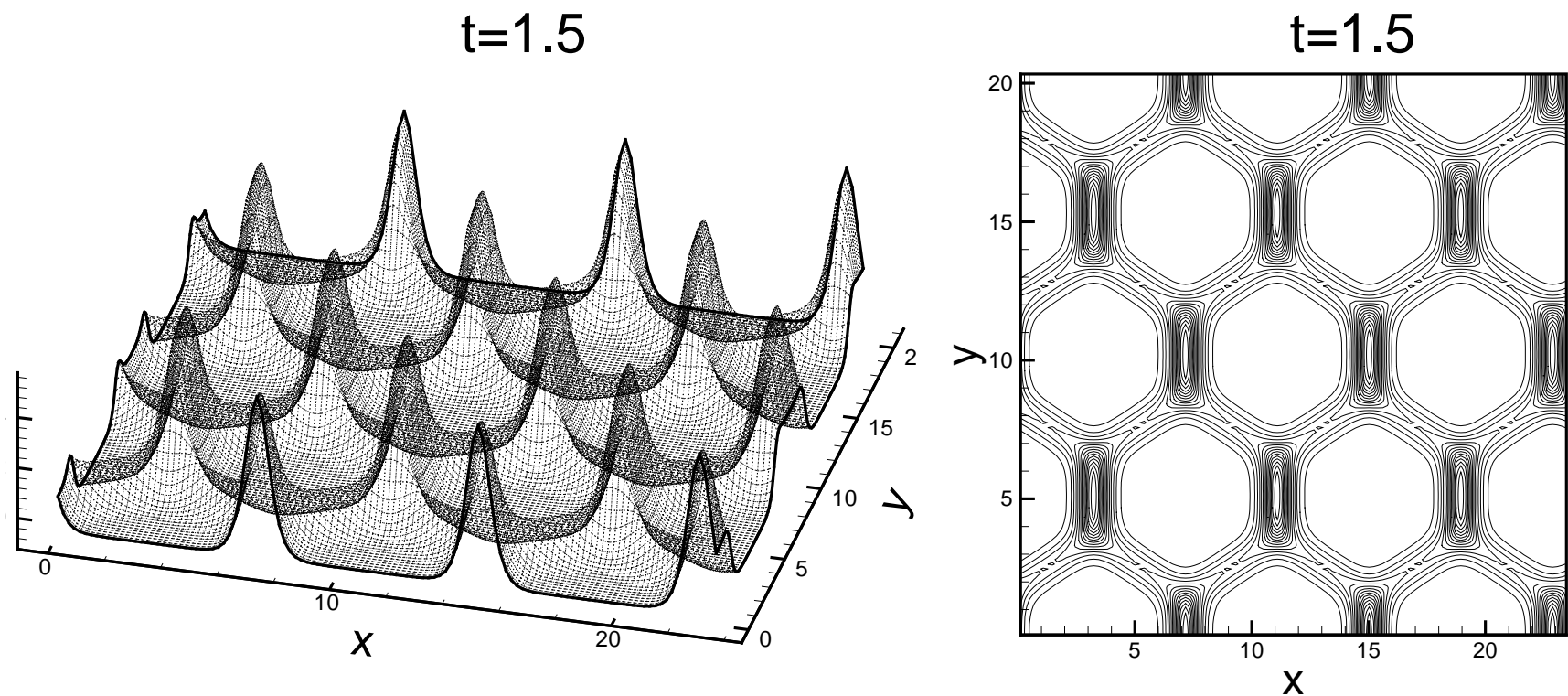


Figure 15: A two-phase solution for the KP-II equation. Periodic boundary condition in both x and y directions in $[0, 6\pi/\mu_1] \times [0, 2\pi/\nu_1]$. P^2 elements with 120×120 uniform cells.

(9) The Zakharov-Kuznetsov (ZK) equation

$$u_t + (3u^2)_x + u_{xxx} + u_{xyy} = 0. \quad (42)$$

We prove the L^2 stability in [Xu and Shu, Physica D 05.](#)

(10) The Camassa-Holm (CH) equation

$$u_t - u_{xxt} + 2\kappa u_x + 3uu_x = 2u_xu_{xx} + uu_{xxx}, \quad (43)$$

where κ is a constant.

We prove the L^2 stability and provide L^2 error estimates for the LDG method in [Xu and Shu, SINUM 08](#).

(11) The Hunter-Saxton (HS) equation

$$u_{xxt} + 2u_x u_{xx} + uu_{xxx} = 0, \quad (44)$$

its regularization with viscosity

$$u_{xxt} + 2u_x u_{xx} + uu_{xxx} - \varepsilon_1 u_{xxxx} = 0, \quad (45)$$

and its regularization with dispersion

$$u_{xxt} + 2u_x u_{xx} + uu_{xxx} - \varepsilon_2 u_{xxxxx} = 0, \quad (46)$$

where $\varepsilon_1 \geq 0$ and ε_2 are small constants.

We design LDG methods and prove the energy stability in [Xu and Shu, SISC 08; JCM 10.](#)

(12) The generalized Zakharov system:

$$iE_t + \Delta E - Nf(|E|^2)E + g(|E|^2)E = 0,$$

$$\epsilon^2 N_{tt} - \Delta(N + F(|E|^2)) = 0,$$

which is originally introduced to describe the Langmuir turbulence in a plasma.

We prove two energy conservations for the LDG method in [Xia, Xu and Shu, JCP 10.](#)

(13) The Degasperis-Procesi (DP) equation

$$u_t - u_{txx} + 4f(u)_x = f(u)_{xxx}, \quad (47)$$

where $f(u) = \frac{1}{2}u^2$. The solution may be discontinuous regardless of smoothness of the initial conditions.

We develop LDG methods and prove L^2 stability for the general polynomial spaces and total variation stability for P^0 elements [Xu and Shu, CiCP 11.](#)

Future work for LDG schemes

Review paper on LDG for higher order PDEs: [Xu and Shu, CiCP 10.](#)

Future work will be carried out in the following directions:

1. Design of stable DG methods for more nonlinear dispersive wave equations and diffusion equations in applications
2. Study of efficient time discretization (preconditioning, multigrid, exponential type time discretization, deferred correction, ...)
3. Error estimates, adaptivity

Recent development and applications

Positivity-preserving finite volume and DG method

The extension of the maximum-principle-preserving and positivity-preserving techniques for hyperbolic equations can be extended to convection-diffusion equations in the following two ways.

A nonstandard finite volume scheme

In Zhang, Liu and Shu (SISC 12), we designed a nonstandard finite volume scheme in order to directly generalize the techniques of Zhang and Shu for maximum-principle-preserving and positivity-preserving for hyperbolic equations to convection-diffusion equations.

Let us look at the heat equation

$$u_t = u_{xx}$$

to see the ideas. Integrating the equation twice we obtain

$$\frac{d}{dt} \int_{x_{i-\frac{1}{2}}}^{x_{i+\frac{1}{2}}} \int_{x-\frac{1}{2}\Delta x}^{x+\frac{1}{2}\Delta x} u(\xi, t) d\xi dx = u(x_{i+1}, t) - 2u(x_i, t) + u(x_{i-1}, t). \quad (48)$$

We define the **double cell averages** of a function $u(x)$ over the intervals

$I_i = [x_{i-\frac{1}{2}}, x_{i+\frac{1}{2}}]$ as

$$\bar{\bar{u}}_i = \frac{1}{\Delta x^2} \int_{x_{i-\frac{1}{2}}}^{x_{i+\frac{1}{2}}} \left(\int_{x-\frac{\Delta x}{2}}^{x+\frac{\Delta x}{2}} u(\xi) d\xi \right) dx.$$

A conservative spatial approximation of (48) with Euler forward time discretization has the form

$$\bar{u}_i^{n+1} = \bar{u}_i^n + \frac{\Delta t}{\Delta x^2} (u_{i+1} - 2u_i + u_{i-1}). \quad (49)$$

A maximum-principle-satisfying finite volume scheme can then be designed as follows:

- Reconstruct the function $u(x)$ from the double cell averages \bar{u}_i , using WENO techniques, at time level n .
- Apply the scaling limiter to the reconstruction polynomial to restrict its distance to \bar{u}_i . The scaling limiter depends only on the evaluation of the unlimited reconstructed polynomial at specific quadrature points.
- Evolve in time using TVD or SSP time discretizations.

It can be proved that this scheme is then uniformly high order accurate and satisfies a strict maximum principle. This result can be generalized to multi-dimensional nonlinear convection-diffusion equations, and to incompressible Navier-Stokes equations in vorticity-streamfunction formulation, on structured meshes.

Reference:

X. Zhang, Y.-Y. Liu and C.-W. Shu, *Maximum-principle-satisfying high order finite volume WENO schemes for convection-diffusion equations*, SIAM Journal on Scientific Computing, v34 (2012), pp.A627-A658.

Piecewise linear DG methods on arbitrary triangular meshes

For regular DG methods, including LDG, DG with penalty formulation, etc., only second order accurate (piecewise linear) DG schemes have been designed to satisfy maximum-principle. The results are contained in [Zhang, Zhang and Shu, JCP 2013](#):

- The same scaling limiter to the piecewise linear DG polynomial to restrict its distance to its cell average. The scaling limiter depends only on the evaluation of the unlimited polynomial at specific quadrature points (for triangles, at the three vertices).
- This method is uniformly second order accurate, works on [any](#) triangular meshes without minimum or maximum angle restrictions, and satisfies strict maximum principle.

This appears to be the first successful result in obtaining uniform second order accurate finite element method on unrestricted triangulations for parabolic equations.

There are attempts to generalize this result to higher order DG methods (Jue Yan).

Reference:

Y. Zhang, X. Zhang and C.-W. Shu, *Maximum-principle-satisfying second order discontinuous Galerkin schemes for convection-diffusion equations on triangular meshes*, Journal of Computational Physics, v234 (2013), pp.295-316.

Multiscale DG method

We consider solving the second order elliptic equation

$$-\nabla \cdot (a^\varepsilon(x) \nabla u) = f \quad \text{in } \Omega \quad (50)$$

with the boundary condition

$$u = 0 \quad \text{on } \partial\Omega, \quad (51)$$

where the coefficient $a^\varepsilon(x)$ is an oscillatory function involving a small scale ε . For example, $a^\varepsilon(x) = a(x, \frac{x}{\varepsilon})$. However, scale separation is **not** required in this framework.

Multi-Scale Approximation Spaces

The DG approximation spaces are constructed as below:

$$S^1 = \{\phi : \nabla \cdot (a^\varepsilon(x) \nabla \phi)|_K = 0\} \quad (52)$$

and

$$S^k = \{\phi : \nabla \cdot (a^\varepsilon(x) \nabla \phi)|_K \in P^{k-2}(K)\} \quad \text{for } k \geq 2 \quad (53)$$

where K denotes the cell in space discretization.

Note: no continuity requirement along element boundary, hence easy to construct in 2D.

1-D case

Now consider the 1-D elliptic problem

$$-(a^\varepsilon(x)u_x)_x = f, \quad 0 \leq x \leq 1 \quad (54)$$

with boundary condition

$$u(0) = u(1) = 0, \quad (55)$$

where

$$0 < \alpha \leq a^\varepsilon(x) \leq \beta < +\infty. \quad (56)$$

1-D multi-scale approximation space:

$$S^k = \left\{ v : v|_{I_j} \in \text{span} \left\{ 1, \int_{x_j}^x \frac{1}{a^\varepsilon(x)} d\xi, \int_{x_j}^x \frac{\xi - x_j}{a^\varepsilon(x)} d\xi, \dots, \int_{x_j}^x \frac{(\xi - x_j)^{k-1}}{a^\varepsilon(x)} d\xi \right\} \right\}.$$

For the IP-DG method, we have the following error estimate:

Theorem (Error Estimates) Let $u(x)$ be the exact solution of the PDE and u_h be the numerical solution of the IP-DG method. There exists a constant C independent of ε such that

$$\|u - u_h\|_{L^2(0,1)} \leq Ch^{k+1}|f|_{H^{k-1}(0,1)}. \quad (57)$$

2-D case

Now consider the 2-D elliptic problem

$$-(a^\varepsilon(x)u_x)_x - (b^\varepsilon(y)u_y)_y = f(x, y), \quad (58)$$

where

$$0 < \alpha \leq a^\varepsilon(x), \quad b^\varepsilon(y) \leq \beta < +\infty. \quad (59)$$

Sample 2-D multi-scale approximation space:

$$S_2^2 = \left\{ v : v|_K \in \text{span} \left\{ 1, \int_{x_K}^x \frac{1}{a(\xi)} d\xi, \int_{y_K}^y \frac{1}{b(\eta)} d\eta, \right. \right. \\ \left. \left. \int_{x_K}^x \frac{\xi - x_K}{a(\xi)} d\xi, \int_{x_K}^x \frac{1}{a(\xi)} d\xi \int_{y_K}^y \frac{1}{b(\eta)} d\eta, \int_{y_K}^y \frac{\eta - y_K}{b(\eta)} d\eta \right\} \right\}.$$

For the IP-DG method, we have the following error estimate:

Theorem (Error Estimates) Let u be the exact solution of the PDE and u_h be the numerical solution of the IP-DG method with $V_h = S_2^1$. There exists a constant C independent of ε such that

$$\|u - u_h\|_{L^2(0,1)} \leq Ch^2 |f|_{L^2(0,1)}. \quad (60)$$

Note: Numerical experiments indicate that the convergence rate holds for k higher than 1 (higher than second order), however we do not have a proof for this yet.

The result can be generalized to equations with curvilinear unidirectional rough coefficients, that is

- At each point, the coefficient is rough (oscillatory) only in one direction, and is much smoother in other directions;
- This oscillatory direction changes smoothly over the space

The biggest advantage for such cases is that we can build explicitly the special DG space basis functions, hence computationally the multiscale DG method is very efficient. This is not possible for continuous finite elements.

Numerical Examples

Example 1. 1-D elliptic problem with

$$a^\varepsilon(x, \varepsilon) = \frac{1}{2 + x + \sin\left(\frac{\sin x}{\varepsilon} \cos x\right)}, \quad f = -\cos x, \quad x \in [0, 1]. \quad (61)$$

Note: No scale separation.

Table 4: L^2 errors and orders of accuracy by the multiscale IP-DG method:
one-dimensional example. S^1

| $\varepsilon = 0.01$ | | | | | $\varepsilon = 0.001$ | | | | |
|----------------------|----------|-----------|----------|-----------|-----------------------|-----------|----------|-----------|--|
| S^1 | | $u - u_h$ | | $q - q_h$ | | $u - u_h$ | | $q - q_h$ | |
| N | error | order | error | order | error | order | error | order | |
| 10 | 1.50E-03 | – | 6.36E-02 | – | 1.44E-03 | – | 6.18E-02 | – | |
| 20 | 3.51E-04 | 2.09 | 2.92E-02 | 1.12 | 3.67E-04 | 1.97 | 3.09E-02 | 1.00 | |
| 40 | 8.95E-05 | 1.97 | 1.50E-02 | 0.96 | 9.26E-05 | 1.99 | 1.54E-02 | 1.00 | |
| 80 | 2.33E-05 | 1.94 | 7.68E-03 | 0.97 | 2.33E-05 | 1.99 | 7.61E-03 | 1.02 | |
| 160 | 5.93E-06 | 1.97 | 3.87E-03 | 0.99 | 5.55E-06 | 2.07 | 3.59E-03 | 1.08 | |

Table 5: L^2 errors and orders of accuracy by the multiscale IP-DG method: one-dimensional example. S^2

| $\varepsilon = 0.01$ | | | | | $\varepsilon = 0.001$ | | | | |
|----------------------|-----------|-------|-----------|-------|-----------------------|-------|-----------|-------|--|
| S^2 | $u - u_h$ | | $q - q_h$ | | $u - u_h$ | | $q - q_h$ | | |
| N | error | order | error | order | error | order | error | order | |
| 10 | 8.39E-06 | – | 5.74E-04 | – | 7.87E-06 | – | 5.60E-04 | – | |
| 20 | 1.10E-06 | 2.94 | 1.38E-04 | 2.05 | 9.75E-07 | 3.01 | 1.40E-04 | 2.00 | |
| 40 | 1.41E-07 | 2.97 | 3.50E-05 | 1.98 | 1.27E-07 | 2.94 | 3.49E-05 | 2.00 | |
| 80 | 1.77E-08 | 3.00 | 8.80E-06 | 1.99 | 1.59E-08 | 2.99 | 8.51E-06 | 2.04 | |
| 160 | 2.21E-09 | 3.00 | 2.20E-06 | 2.00 | 1.96E-09 | 3.02 | 2.14E-06 | 1.99 | |

Example 2. 2-D elliptic problem with

$$a(x) = a^\varepsilon(x, \varepsilon) = \frac{1}{4 + x + \sin\left(\frac{\sin x}{\varepsilon} \cos x\right)},$$

$$b(y) = b^\varepsilon(y, \varepsilon) = \frac{1}{4 + y + \sin\left(\frac{\sin y}{\varepsilon} \cos y\right)}, \quad f = x + y.$$

An explicit formula for the exact solution is unavailable, and we are using the numerically obtained reference solution.

Note: Again there is no scale separation.

Table 6: L^2 errors and orders of accuracy by the multiscale IP-DG method:
two-dimensional example. S_2^1 .

| $\varepsilon = 0.01$ | | | $\varepsilon = 0.005$ | | |
|----------------------|----------|-------|-----------------------|-------|--|
| N | error | order | error | order | |
| 10 | 4.00E-02 | — | 6.45E-02 | — | |
| 20 | 1.26E-02 | 1.67 | 1.80E-02 | 1.84 | |
| 40 | 3.54E-03 | 1.83 | 4.83E-03 | 1.90 | |
| 80 | 9.34E-04 | 1.92 | 1.22E-03 | 1.98 | |

Table 7: L^2 errors and orders of accuracy by the multiscale IP-DG method:
two-dimensional example. S_2^2 .

| $\varepsilon = 0.01$ | | | $\varepsilon = 0.005$ | | |
|----------------------|----|----------|-----------------------|----------|-------|
| S_2^2 | N | error | order | error | order |
| | 10 | 1.23E-03 | – | 1.34E-03 | – |
| | 20 | 1.81E-04 | 2.76 | 1.84E-04 | 2.87 |
| | 40 | 2.64E-05 | 2.78 | 2.57E-05 | 2.84 |
| | 80 | 3.69E-06 | 2.84 | 3.55E-06 | 2.85 |

References:

- [1] L. Yuan and C.-W. Shu, *Discontinuous Galerkin method based on non-polynomial approximation spaces*, Journal of Computational Physics, v218 (2006), pp.295-323.
- [2] W. Wang, J. Guzmán and C.-W. Shu, *The multiscale discontinuous Galerkin method for solving a class of second order elliptic problems with rough coefficients*, International Journal of Numerical Analysis and Modeling., v8 (2011), pp.28-47.
- [3] Y. Zhang, W. Wang, J. Guzmán and C.-W. Shu, *Multi-scale discontinuous Galerkin method for solving elliptic problems with curvilinear unidirectional rough coefficients*, submitted to Journal of Scientific Computing.

Energy conserving LDG methods for second order wave equations

We consider the second order wave equation

$$u_{tt} = u_{xx}, \quad \text{in } [a, b] \times [0, T], \quad (62)$$

subject to the initial conditions

$$u(x, 0) = u_0(x), \quad u_t(x, 0) = v_0(x). \quad (63)$$

This equation can be converted to a standard first order hyperbolic system. DG scheme for such a system can be designed based on the standard upwind numerical flux. This DG scheme has the following features:

- It is energy dissipative: the total energy decays with time.
- It is optimal $(k + 1)$ -th order convergent with piecewise polynomials of degree k .

For nonlinear problems with discontinuous solutions, upwinding and its numerical dissipation are good to use. The resulting scheme is not only optimal convergent for smooth solutions but also stable for discontinuous solutions, with the capability of confining the errors in a small neighborhood of the discontinuity.

On the other hand, if we use a central numerical flux, then the resulting DG scheme has the following features:

- It is energy conserving: the total energy is constant in time.
- It is sub-optimal k -th order convergent with piecewise polynomials of degree k for some k .

Besides its sub-optimal convergence rate, the DG scheme with central flux is also very oscillatory when the solution becomes discontinuous.

However, if the exact solution is smooth and we would like to simulate the wave propagation over a long time period, then energy conserved numerical methods have advantages. We will show numerical evidence later. For first order hyperbolic systems, it is difficult to obtain DG schemes which are energy conservative and also optimal order convergent. Chung and Engquist (SINUM 06; SINUM 09) have proposed an optimal, energy conserving DG method for the first order wave equation using staggered grids.

On the other hand, we can directly approximate the second order wave equation by an LDG method. Find $u_h, q_h \in V_h^k$, such that

$$\int_{I_j} (u_h)_{tt} v dx + \int_{I_j} q_h v_x dx - (\hat{q}_h v^-)_{j+\frac{1}{2}} + (\hat{q}_h v^+)_{j-\frac{1}{2}} = 0 \quad (64)$$

$$\int_{I_j} q_h w dx + \int_{I_j} u_h w_x dx - (\hat{u}_h w^-)_{j+\frac{1}{2}} + (\hat{u}_h w^+)_{j-\frac{1}{2}} = 0 \quad (65)$$

for all test functions $v, w \in V_h^k$. When the numerical fluxes are chosen as the alternating fluxes:

$$\hat{q}_h = q_h^-, \quad \hat{u}_h = u_h^+, \quad (66)$$

we obtain both energy conservation and optimal L^2 convergence.

This LDG scheme can be generalized to second-order wave equation in heterogeneous media, that is, wave equation with variable coefficients which are possibly discontinuous, in multi-dimensions.

References:

Y. Xing, C.-S. Chou and C.-W. Shu, *Energy conserving local discontinuous Galerkin methods for wave propagation problems*, Inverse Problems and Imaging, to appear.

C.-S. Chou, C.-W. Shu and Y. Xing, *Optimal energy conserving local discontinuous Galerkin methods for second-order wave equation in heterogeneous media*, submitted to Journal of Computational Physics.

We numerically investigate the long time evolution of the L^2 error of the LDG method, in comparison with an IPDG method (Grote et al, SINUM 06) which conserves a specifically defined energy but not the usual energy. We consider again the wave equation

$$u_{tt} = u_{xx}, \quad x \in [0, 2\pi]$$

with a periodic boundary condition $u(0, t) = u(2\pi, t)$ for all $t \geq 0$, and initial conditions $u(x, 0) = e^{\sin x}$, $u_t(x, 0) = e^{\sin x} \cos x$. This problem has the exact solution $u = e^{\sin(x-t)}$.

The LDG and IPDG methods are implemented with a uniform mesh with N cells, and the leap-frog time discretization, with $\Delta t = 0.6h^2$. In order to examine the potential shape difference resulted from long time integration, both methods are run until $T = 1000$, with finite element spaces P^2 and P^3 , and $N = 40, 80$, respectively.

In Fig. 16, the time evolution of L^2 errors of both schemes are shown. The L^2 errors of both schemes grow in a linear fashion, but the slope for IPDG method is much larger than that for LDG method, which almost stays as constant and is close to zero. The errors are plotted in log scale for easy visualization. From the figure, one can see that for LDG method, the level of the errors are reduced by refining the mesh from $N = 40$ to $N = 80$, but the mesh refinement does not substantially reduce the errors of IPDG method due to the rapid growth.

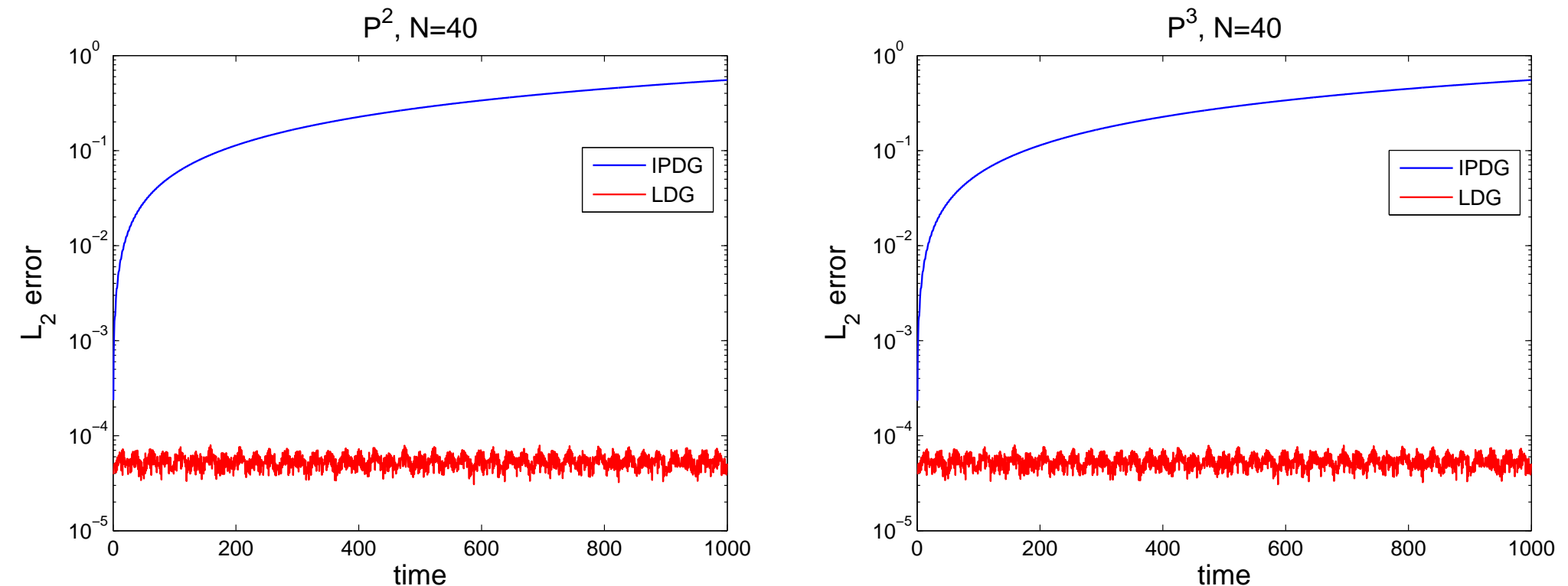


Figure 16: Time history until $T = 1000$ of the L^2 error of the numerical approximations obtained from the LDG and IPDG methods with $k = 2, 3$ and a uniform mesh with 40 cells. The L^2 error on y -axis are presented in log scale.

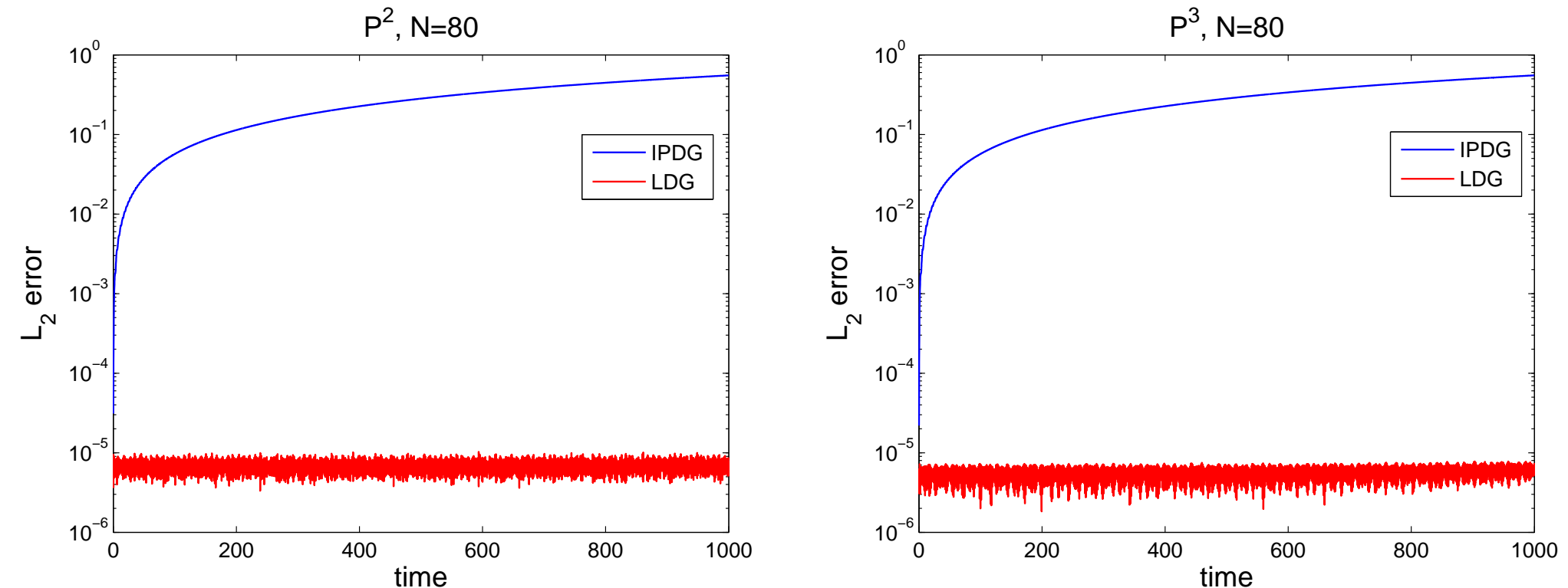


Figure 17: Time history until $T = 1000$ of the L^2 error of the numerical approximations obtained from the LDG and IPDG methods with $k = 2, 3$ and a uniform mesh with 80 cells. The L^2 error on y -axis are presented in log scale.

It can be observed from Fig. 16 that, up to $T = 1000$, the L^2 error of IPDG method is greater than 10^{-1} , and this large error can easily be visualized by directly comparing the solutions of both methods. Fig. 18 displays the exact solution (red), the solution of LDG method (green) and the solution of IPDG method (blue) at $T = 1000$, for spaces P^2 and P^3 with $N = 40$. It can be seen that solution of LDG method overlaps with the exact solution, while the solution of IPDG method preserves the shape but has a phase shift.

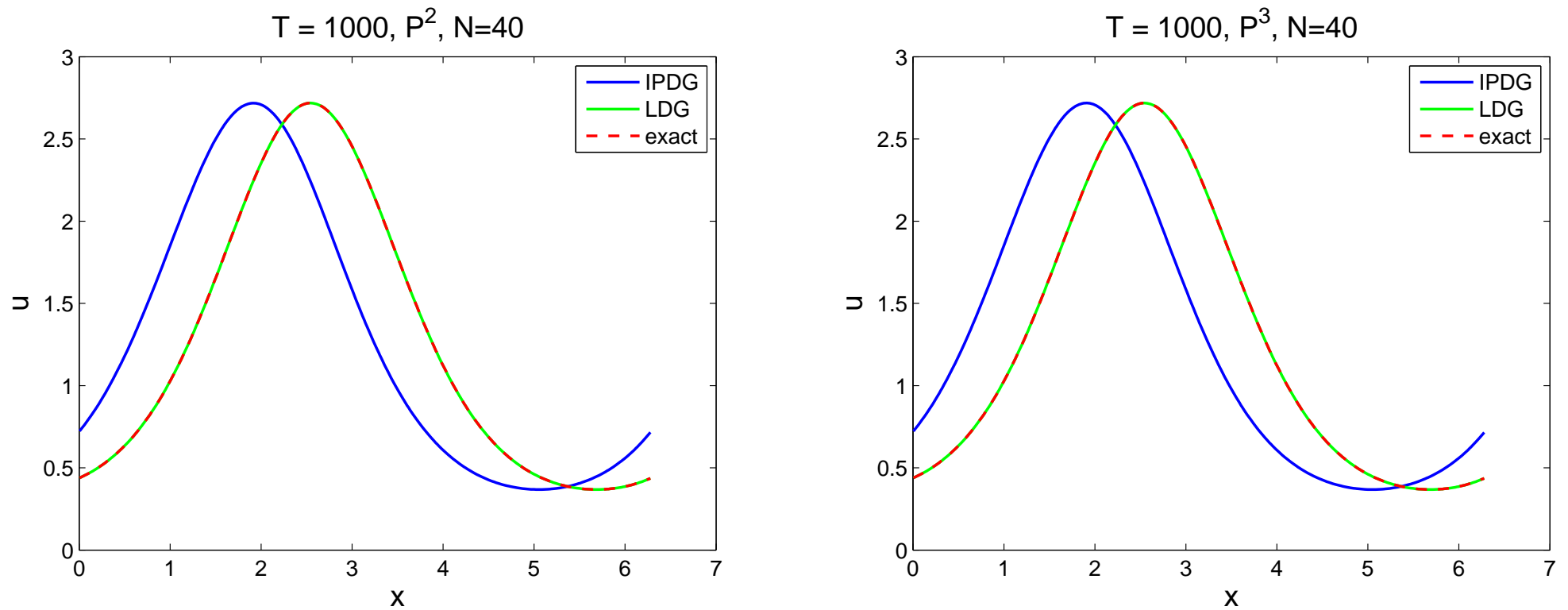


Figure 18: Numerical approximations of the wave equation using LDG and IPDG methods. Comparison is made at $T = 1000$ with $k = 2, 3$ and $N = 40$.

DG METHOD II: PDEs WITH HIGHER ORDER DERIVATIVES

The End

THANK YOU!